Land-cover change alters stand structure, species diversity, leaf functional traits, and soil conditions in Cambodian tropical forests

Chansopheaktra Sovann[1,2], Torbern Tagesson[1], Patrik Vestin[1], Sakada Sakhoeun[3], Soben Kim[4], Sothea Kok[2], Stefan Olin[1]

[1]Department of Physical Geography and Ecosystem Science, Lund University, Sölvegatan 12, 22362 Lund, Sweden
[2]Department of Environmental Science, Royal University of Phnom Penh, Phnom Penh, 120404, Cambodia
[3]Provincial Department of Environment, Ministry of Environment, Siem Reap, 171202, Cambodia
[4]Faculty of Forestry, Royal University of Agriculture, Phnom Penh, 120501, Cambodia

Correspondence to: Chansopheaktra Sovann (chansopheaktra.sovann@nateko.lu.se)

Abstract. Given the severe land-use and land-cover change pressure on tropical forests and the high demand for field observations of ecosystem characteristics, it is crucial to collect such data both in pristine tropical forests and in the converted deforested land-cover classes. To gain insight into the ecosystem characteristics of pristine tropical forests, regrowth forests, and cashew plantations, we established an ecosystem monitoring site in Phnom Kulen National Park, Cambodia. Here, we present the first observed datasets at this site of forest inventories, leaf area index, leaf traits of woody species, a fraction of intercepted photosynthetically active radiation, and soil and meteorological conditions. Using these data, we aimed to assess how land-cover change affects stand structure, species diversity, leaf functional traits, and soil conditions among the three land-cover classes, and to evaluate the feasibility of locally calibrated diameters at breast height (*DBH*) and tree height (*H*) allometries for improving aboveground biomass estimation. We found significant differences in these ecosystem characteristics, caused by the anthropogenic land-cover conversion, which underlines land-cover change's profound impact on stand structure, species diversity, leaf functional traits, and soil conditions in these tropical forest regions. Our results further demonstrated the feasibility of locally updating aboveground biomass estimates using power-law functions based on relationships between *DBH* and *H*. These datasets and findings can contribute to enriching tropical forest research databanks and supporting sustainable forest management.

Keywords: tropical forest, forest ecosystem, forest inventory, biomass, Kulen, Cambodia.

Graphical abstract:

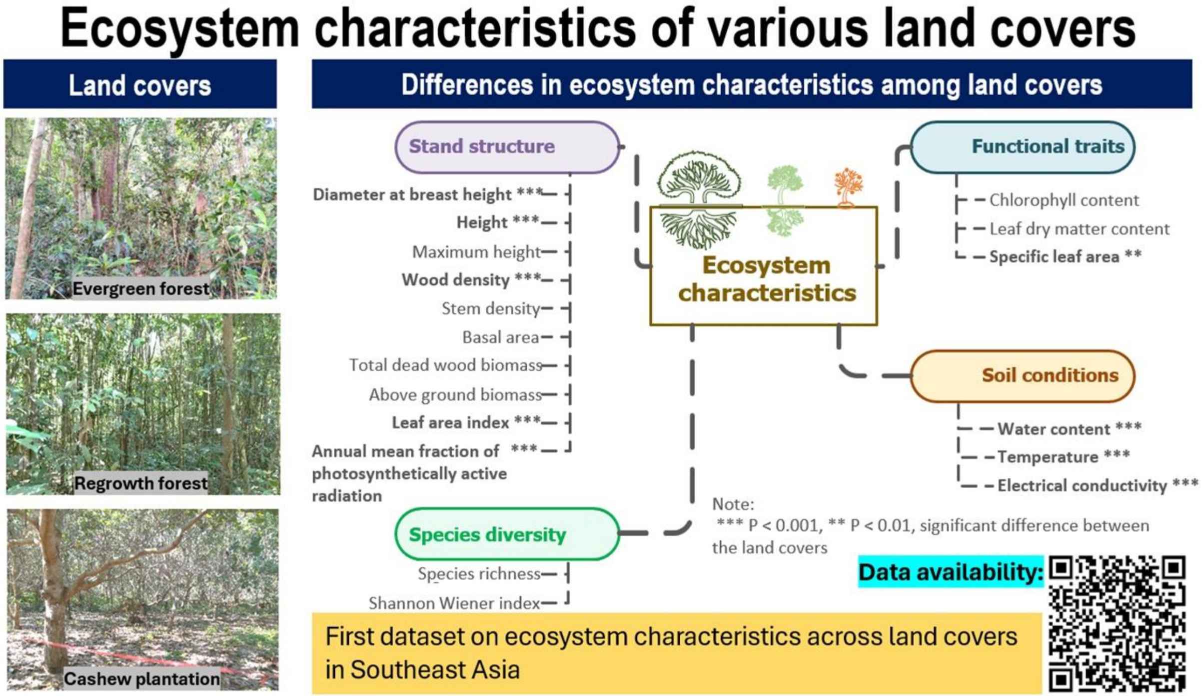

Ecosystem characteristics of various land covers

Land covers

Evergreen forest

Regrowth forest

Cashew plantation

Differences in ecosystem characteristics among land covers

Ecosystem characteristics

Stand structure

- **Diameter at breast height *****
- **Height *****
- Maximum height
- **Wood density *****
- Stem density
- Basal area
- Total dead wood biomass
- Above ground biomass
- **Leaf area index *****
- **Annual mean fraction of photosynthetically active radiation *****

Species diversity

- Species richness
- Shannon Wiener index

Functional traits

- Chlorophyll content
- Leaf dry matter content
- **Specific leaf area ****

Soil conditions

- **Water content *****
- **Temperature *****
- **Electrical conductivity *****

Note:
*** P < 0.001, ** P < 0.01, significant difference between the land covers

Data availability:

First dataset on ecosystem characteristics across land covers in Southeast Asia

1 Introduction

Tropical forests cover approximately 14 % of the Earth's surface (Fichtner and Härdtle, 2021) and contribute significantly to global terrestrial biodiversity (Giam, 2017) and biogeochemical cycles (Males et al., 2022). Tropical forests produce at least 30 % of the global terrestrial net primary production (Townsend et al., 2011; Wright, 2013) and account for approximately 70 % of the global gross carbon sink (Pan et al., 2024). In addition, they play a critical role in regulating hydrological cycles on a continental scale (Gloor et al., 2013). Tropical forests have been under severe anthropogenic pressures from agricultural land expansion, resource exploitation (logging, mining), and urbanization (Gardner et al., 2009; Laurance et al., 2014). Such disturbances have resulted in significant structural and functional degradation in tropical forests, highlighting the urgent need to assess how land-cover change alters key ecosystem characteristics (Barlow et al., 2016).

Southeast Asia, though harbouring roughly 15 % of the world's tropical forests (Stibig et al., 2014), has suffered the highest global deforestation rates over the past 15 years (Miettinen et al., 2011). This alarming trend threatens over 40 % of the region's biodiversity by 2100 (Sodhi et al., 2004). The forests are mainly disturbed by timber harvesting (Pearson et al., 2017), slash-and-burn agriculture, and agricultural plantations as a consequence of fulfilling global demands for timber production and agricultural commodities, especially rubber, cashew, oil palm, Eucalyptus and Acacia (Phompila et al., 2014; Grogan et al., 2015; Chen et al., 2016; Johansson et al., 2020). In addition to primary forests, secondary forests that regenerate after clear-cutting or other ecosystem disturbances are also important for protecting biodiversity and assuring the availability of ecosystem services and goods (Tito et al., 2022). While the ecological consequences of forest conversion are broadly recognized, relatively few studies have comprehensively examined how transitions from primary to secondary forests and plantations influence multiple ecosystem characteristics, particularly through detailed field-based observations that may inform our understanding of ecosystem functioning.

Tropical forests demonstrate remarkable ecological complexity, with high diversity in stand structure, species composition, and functional traits shaped by heterogeneous environments and varied disturbance histories (Manuel Villa et al., 2020). This complexity leads to highly site-specific and often inconsistent ecosystem characteristics and responses, making it difficult to generalize the impacts of land-cover change across regions (Wang et al., 2022). A parallel challenge in tropical forest research is the accurate estimation of aboveground biomass (*AGB*), a key metric for assessing carbon stocks. Most studies rely on generalized allometric models developed under different ecological conditions, assuming similarity in forest structure, composition, and wood density, which these assumptions rarely hold in structurally diverse tropical forests (Vieilledent et al., 2012). These limitations introduce substantial uncertainty when models are applied across sites (Ketterings et al., 2001b). The lack of locally calibrated relationships between diameter at breast height (*DBH*) and tree height (*H*), wood density (*WD*), and the scarcity of direct destructive sampling further contribute to estimation errors, highlighting the need for site-specific approaches that reflect local variation in forest structure and composition.

In the context of tackling the current challenges of global land cover change, it is necessary to conduct field observations in order to investigate the responses of ecosystems to changing environmental conditions on fine spatial and temporal scales.

Field observations of key ecosystem characteristics such as forest inventory, leaf functional traits, leaf area index (*LAI*), fraction of photosynthetically active radiation (*fPAR*), and soil conditions provide crucial insights into ecosystem functions and services, including vegetation productivity, carbon sequestration, hydrological cycle, ecosystem stability and resilience to disturbances, nutrient reservoir capacity, and the abundance of habitats of organisms (Naeem et al., 1994; Hector, 1998; Cardinale et al., 2012; Chen et al., 2016; Liang et al., 2016; Parisi et al., 2018b; Woodall et al., 2020). In addition, the field data on leaf functional traits, *LAI*, and *fPAR* are important for the parameterization and evaluation of remote sensing products and dynamic vegetation models, essential for modelling and upscaling ecosystem responses to anthropogenic disturbances and climate change (Feng et al., 2018; Fang et al., 2019; Pei et al., 2022). Recognizing the significant role and high demand for field observations of ecosystem characteristics, open data repositories such as FLUXNET, ICOS Carbon Portal, SpecNet, and the TRY database have been established to facilitate data sharing (Gamon et al., 2010; Kattge et al., 2020; Pastorello et al., 2020). Despite those global initiatives, observed data from tropical forests that support multi-class, pairwise comparisons for capturing ecosystem changes across gradients of forest degradation and land-use conversion remain limited. This gap is especially critical in Southeast Asia, where rapid forest-to-agriculture transitions threaten key ecosystem functions, and understanding these ecosystem changes is essential for informing evidence-based conservation and restoration strategies (Fan et al., 2024).

Within this context, Phnom Kulen National Park (Kulen) in Cambodia emerges as a critical landscape for investigating ecosystem responses to land cover change. Kulen is a hotspot for ecosystem service provisioning in Cambodia, mainly for water supply, potential carbon sink, and cultural services (Jacobson et al., 2022; Kim et al., 2023). It is the origin of the Khmer Empire and contains numerous archaeological sites. The stream water from the mountain is not only used to support local livelihoods in water supply and irrigation downstream (Somaly et al., 2020). It is also the primary water source to recharge surface water and groundwater aquifers in the Angkor Wat, UNESCO World Heritage Site. Hence, the area is of high importance to ensure that the temples' foundations remain stable and maintain their surrounding forest ecosystem (Hang et al., 2016). However, previous studies revealed that the forestland in and around Kulen has been disturbed, largely driven by agricultural expansion, particularly the spread of cashew plantations (Chim et al., 2019; Sovann et al., 2025).

Given increasing concerns about land use and land cover change threatening the high-value ecosystem functions of tropical forests like those in Kulen, our study aims to gain insight into the impact of land-cover conversion on key ecosystem characteristics. Specifically, our first objective is to assess the differences in stand structure, species diversity, leaf functional traits, and soil conditions between pristine tropical forests and the land cover the deforested regions are converted into (regrowth forests and cashew plantations). We hypothesise that there will be a reduction in stand structural complexity, species composition, and leaf functional traits, and a marked change in soil conditions. Additionally, our second objective is to evaluate the feasibility of locally updating aboveground biomass estimates by applying power-law functions derived from site-specific relationships between diameter at breast height and tree height, with the hypothesis that locally calibrated *DBH-H* relationships will have a substantial effect on estimated aboveground biomass compared to regional or generalized allometric models. To test these hypotheses, we will analyse a novel in situ dataset collected from pristine tropical forests, regrowth forests, and cashew plantations at a newly established ecosystem monitoring site in Phnom Kulen National Park, Cambodia.

2 Materials and Methods

2.1 Study area and selection of plots

The selected study area is the Phnom Kulen National Park located in the Siem Reap Province in north-west Cambodia (Fig. 1). It covers 37,380 ha predominantly on Jurassic-Cretaceous sandstone plateaus with the highest peak of 496 m (Matschullat, 2014; Geissler et al., 2019). In 2021, 72 % of Phnom Kulen National Park was forested, dominated by nearly intact tropical evergreen forests (EF) (30 %) and forests that regrow naturally after clear-cutting (RF) (7 %). The remaining 35 % of forest cover consisted of semi-evergreen, deciduous, and bamboo stands. Non-forest areas were dominated by household-scale cashew plantations (CP) (15 %), with the remaining 13 % consisting of croplands, paddy fields, settlements, and tree and rubber plantations (Sovann et al., 2025).

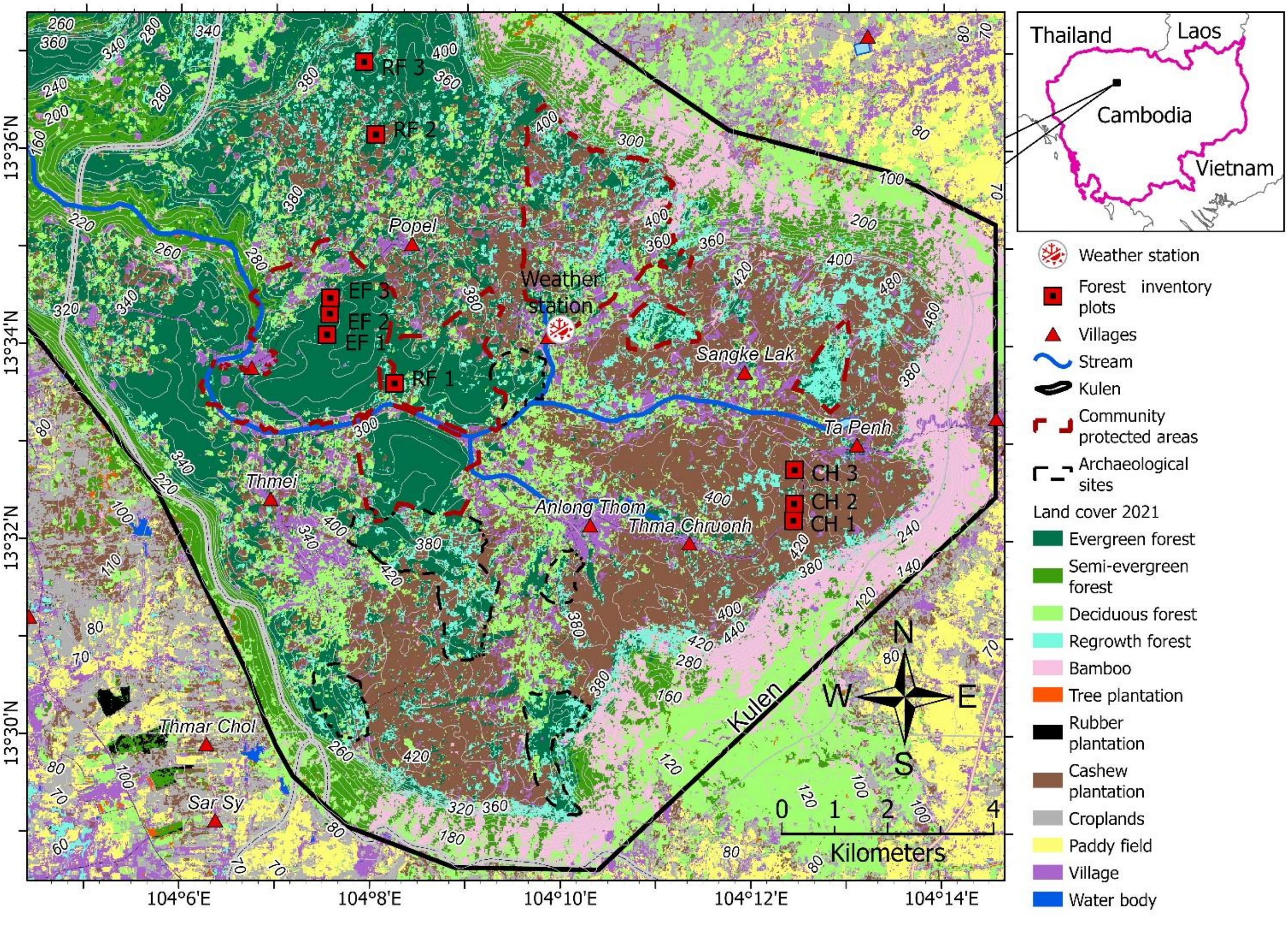

Figure 1. The locations of the nine forest inventory plots and the meteorological station in the Phnom Kulen National Park, Cambodia. Note: the background land cover 2021 was derived from Sovann et al. (2025).

Nine forest inventory plots were established in Kulen in December 2020, three within each of the EF, RF, and CP land-cover classes (Fig. 1, Table 1, Fig. S1.1), with a minimum separation of 250 meters to capture stand structure variation for each land-cover class. The EF plots represented tropical evergreen forests with no clear-cut history. The RF plots were dominated by at least 10-year-old natural regrowth forests, RF1 was clear-cut in 2009, while RF2 and RF3 experienced timber harvesting, burning, and fuelwood collection from 2006 to 2013. The CP plots were permanent rainfed cashew plantations, with cashew trees planted in 2013 in CP1 and in 2012 for the other two.

Table 1. Characteristics of the forest inventory plots in Phnom Kulen National Park. Note: EF = evergreen forests, RF = regrowth forests, and CP = cashew plantations. Data source: Soil type and geology data from Matschullat (2014). Disturbance history information is obtained from field observation, discussion with local people, and combining with the Global Forest Change dataset of Hansen et al. (2013) and LandTrendr Pixel Time Series Plotter tool of Kennedy et al. (2018).

Plot ID	Latitude, Longitude	Elevation (m)	Soil type	Disturbance history
EF1	N 13° 34' 12.4680" E 104° 7' 18.6096"	331	Acid Lithosols	No clear-cut history; affected by wind disturbance and human collection of wild honey, lychee, and other wild fruits in 2006, 2012, and 2014. Fewer large tree stands and lower vegetation cover density compared to EF2 and EF3.
EF2	N 13° 34' 25.3452" E 104° 7' 20.2872"	349	Acid Lithosols	No clear-cut history; past disturbances include cutting one lychee tree for fruit harvesting in 2022.
EF3	N 13° 34' 35.0508" E 104° 7' 20.6148"	339	Acid Lithosols	No clear-cut history; a wind-driven disturbance occurred in 2023.
RF1	N 13° 33' 42.6132" E 104° 8' 1.2408"	331	Red-yellow podzols	Evergreen forest clear-cut in 2009.
RF2	N 13° 36' 15.6924" E 104° 7' 48.8928"	371	Acid Lithosols	Timber harvesting, burning, and fuelwood collection of an evergreen forest from 2006 to 2013.
RF3	N 13° 37' 0.3612" E 104° 7' 41.358"	401	Acid Lithosols	Timber harvesting, burning, and fuelwood collection of an evergreen forest from 2006 to 2013.
CP1	N 13° 32' 18.8988" E 104° 12' 12.5568"	429	Red-yellow podzols	Cashew plantation established in 2013.
CP2	N 13° 32' 29.3100" E 104° 12' 13.0284"	422	Red-yellow podzols	Cashew plantation established in 2012.
CP3	N 13° 32' 50.1864" E 104° 12' 13.1544"	430	Red-yellow podzols	Cashew plantation established in 2012.

2.2 Data collection

2.2.1 Forest inventory

The forest inventory was performed by following the standard method of the National Forest Inventory of Cambodia (Than et al., 2018). Each plot was designed as a rectangle with 50 m x 30 m long edges in the south-north and west-east directions. The plots were further subdivided into five subplots with the following dimensions: 2 m x 2 m, 5 m x 5 m, 10 m x 10 m, 30 m x 15 m, and 30 m x 50 m (Fig. S1.2). In the 2 m × 2 m subplots, seedlings with diameters at breast height (*DBH*, 1.3 m above ground) of less than 1 cm were recorded. In the 5 m x 5 m, 10 m x 10 m, 30 m x 15 m, and 30 m x 50 m subplots, trees with *DBH* ranges of 1–5 cm, 5–15 cm, 15–30 cm, and greater than 30 cm were measured, respectively.

For seedlings, we only recorded the total numbers of each species. For the *DBH* range of 1–5 cm, we noted the *DBH*, tree height, species, local name (Khmer), and position of each tree. For trees with a *DBH* greater than 5 cm, we collected the same data as for trees with a *DBH* of 1–5 cm, plus bole height (the height from the ground to the first main lowest stem), health (healthy or infected), quality (straight, bent, or crooked stem), origin (natural or planted), and stump diameter and height (measured 15 cm above ground for annual tree growth monitoring).

Deadwood is a significant indicator of decomposition and nutrient cycling processes in a forest ecosystem (Shannon et al., 2021). Data on lying and standing deadwood with a *DBH* greater than 10 cm in the 30 m x 15 m subplots were also collected. The deadwood decomposition levels were classified into five scales, based on harmonizing the scaling systems of the National Forest Inventory of Sweden (Swedish NFI, 2019) and Cambodia (Than et al., 2018) (Table S1.1). For standing deadwood, we recorded their species, local name, location, height, and decomposition level. For lying deadwood, we counted the number of pieces and measured their lengths, base and tree diameters, and decomposition levels.

2.2.2 Leaf sample collection and measurement

A total of 453 leaf samples from 30 woody species were collected inside and 500 m around the forest inventory plots in December 2019 and August 2022. Each species was represented by five to 47 leaf samples. Each leaf's fresh mass, chlorophyll content, and photo were taken in the field. A Chlorophyll Meter (SPAD 502 Plus; Konica Minolta Sensing Inc., Japan) was used in situ to measure chlorophyll content five times on each leaf surface to retrieve a leaf mean value. The given measurement unit was in SPAD value (Soil Plant Analysis Development) and later converted to chlorophyll a and b content (*Chl*) in µg cm^{-2} (Coste et al., 2010). We obtained fresh leaf mass by weighting in the field and leaf dry mass by oven-drying the leaves at 60 °C until the leaf mass remained constant (oven-dried for at least three days) (Garnier et al., 2001). The leaf photos were used for estimating leaf lengths and areas using ImageJ (Schindelin et al., 2012; Schneider et al., 2012).

2.2.3 Meteorological and photosynthetically active radiation data

A meteorological station was installed in an open area to continuously record meteorological conditions, and incoming photosynthetically active radiation (*PAR*) for the wider area (the Kulen National Park). Data were sampled at one minute intervals and stored as 15 minute averages (sum for rainfall). The installation was done in November 2020 in Khnang Phnom Commune, Svay Luer District, Siem Reap Province, at 13° 34' 16.1148" N, 104° 9' 45.6768" E, and an altitude of 314 m above mean sea level. The station has one Atmos 41 meteorological station (Meter Group Inc. WA, USA), installed 2.2 m above ground level, measuring rainfall, wind speed, wind direction, global radiation, atmospheric pressure, and air temperature. Additionally, four *PAR* sensors (SQ-110-SS, Apogee Instruments, Inc., UT, USA) were positioned 2 m above the ground to record incoming *PAR* (PAR_{inc}) (Fig. S2.1).

Six additional loggers with five *PAR* sensors (SQ-521-SS and SQ-110-SS, Apogee Instruments, Inc., UT, USA) and one TEROS 12 soil moisture sensor each (Meter group Inc. WA, USA), collecting data at a 15 minute mean timestep, were installed in six of the forest inventory plots in April 2022. The soil moisture sensors were installed at a depth of 20 cm to measure soil water content (*SWC*), soil temperature (*Ts*), and soil electrical conductivity (*ECs*). Two loggers were placed in each land-cover class (EF, RF, and CP). The selection of plots in each land-cover class was based on previous measurements of leaf area index and the loggers were placed at the plots with the highest and lowest *LAI* for each land cover, respectively. Thus, the selected plots for installing *PAR* sensors were EF1, EF3, RF1, RF3, CP2, and CP3 (Fig. 1). The *PAR* sensors were placed with one in the centre of the plot and the other four placed 15 ± 1 m apart at 30°, 150°, 220°, and 330° from the north. In cases of unfavourable field conditions, such as high termite nests or being too close to a tree, the locations were adjusted 0.5–1 m east or west of the planned position. Each *PAR* sensor was mounted on 1.3 m poles to record *PAR* below canopy data. We calculated the fraction of *PAR* intercepted by the stand canopy for each plot using Eq. (1) (Olofsson and Eklundh, 2007). Each TEROS 12 soil moisture sensor was installed at a depth of 20 cm in the middle of the six plots to measure *SWC*, *T*s, and *EC*s. The data of *fPAR* and soil conditions from two plots within the same land-cover classes were averaged to represent those classes.

$$fPAR = \frac{(PAR_{\mathrm{inc}} - PAR_{\mathrm{below}})}{PAR_{\mathrm{inc}}} \tag{1}$$

Where PAR_{inc} and PAR_{below} are photosynthetically active radiation above and below canopy (µmol $\mathrm{m}^{-2}\,\mathrm{s}^{-1}$). $fPAR$ is in percentage.

2.2.4 Leaf area index measurements

We measured each plot's total one-sided leaf surface area per unit ground area, *LAI*, using a LAI-2000 Plant Canopy Analyzer (LI-COR, NE, USA). The measurements were conducted six times across two seasons: four times during the dry season (November/December 2019, November 2020, December 2020, and March 2021) and twice during the rainy season (September 2020 and June 2021). The measurements were taken both at ground level to capture the total *LAI* (LAI_{T}) and at breast height to specifically assess tree canopy *LAI* (LAI_{C}) within two diagonal transects across the 50 m x 30 m rectangular plots. On each measurement occasion, we collected between 32 and 75 samples, except for the ground-level measurements of the RF3 plot in December 2020, where only ten samples were collected due to technical issues.

2.3 Data analysis

2.3.1 Species diversity

We investigated the species diversity of various land covers by calculating species richness (S_R) and the Shannon-Wiener index (S_H) (Shannon, 1948). The S_R was determined by summing the number of tree species in each plot. The S_H is commonly used to quantify species richness and evenness in a community by representing the number of species and how equally individuals are distributed among them (Hill, 1973). The value of S_H increases as the number of species and the degree of evenness increase. The S_H was calculated by:

$$S_{\mathrm{H}} = -\sum_{i=1}^{n} P_{\mathrm{i}} \ln(P_{\mathrm{i}}) \tag{2}$$

Where S_H is Shannon-Wiener index (unitless), P_i is a proportion of i species in a community (unitless), and n is the number of species in a plot (unitless). We calculated the S_R and S_H at the plot level and then averaged the values for each land-cover class.

2.3.2 Functional traits and diversity

We computed the specific leaf area (*SLA*) for each of the 453 leaf samples as the ratio of leaf area to leaf dry mass. Likewise, leaf dry matter content (*LDMC*) was calculated by the ratio of dry leaf mass to fresh leaf mass (Garnier et al., 2001; Akram et al., 2023). We estimated the trait community-weighted means and standard deviations of SLA_{cwm}, $LDMC_{\mathrm{cwm}}$, and Chl_{cwm} to represent ecosystem functions and their diversity at the land-cover level (Garnier et al., 2004; Leoni et al., 2009; Wang et al., 2020) with:

$$T_{\mathrm{cwm}} = \frac{\sum_{i=1}^{n} W_{\mathrm{i}} T_{\mathrm{i}}}{\sum_{i=1}^{n} W_{\mathrm{i}}} \tag{3}$$

Where T_{cwm} is trait community-weighted mean for *SLA*, *LDMC*, or *Chl*, T_i is the species-specific trait value tree i, n is total number of trees, W_i is the weight (volume based) value of the tree, assuming that larger trees have a greater impact on the ecosystem function (Chave et al., 2005; Feldpausch et al., 2011). Before computing T_{cwm} for each trait, we addressed missing species traits within each plot by first taking values from a different plot with the same land-cover class. If unavailable, we used values from the same species across all nine plots, followed by values from the genus and family levels. When multiple genera or families were available, we averaged the values. If neither was available, we used the mean trait value of the plot.

2.3.3 Stand structural attributes

We examined the differences in *DBH*, *H*, basal area (*BA*), aboveground biomass, and deadwood biomass (*DWB*) for the various land-cover classes to characterize stand structure attributes. Deadwood volumes (V_{DW}, m^3) for each bole were determined by Smalian's equation:

$$V_{DW} = (\pi\, H_{\mathrm{b}})\, \frac{\left(D_{\mathrm{base}}^2 + D_{\mathrm{top}}^2\right)}{8} \tag{4}$$

Where D_{base} and D_{top} are diameters at base and top (m), and H_{b} is the length/height of the trunk (m).

Deadwood biomass was then received by multiplying V_{DW} with a mean deadwood density of 0.45 g cm^{-3} (Kiyono et al., 2007). Total *DWB* was computed plot-wise by taking the sum of lying and standing *DWB*. *DWB* for each land-cover class was calculated as the average of the total *DWB* across the plots within that land-cover class.

Basal area was determined plot-wise by combining the *DBH* of all living trees within a plot:

$$BA = \sum_{i=1}^{n} \pi \left(\frac{DBH_{\mathrm{i}}}{2}\right)^2 \left(\frac{10^4}{A_{\mathrm{i}}}\right) \tag{5}$$

Where BA is a plot-wise total basal area of all living trees (m^2 ha^{-1}), n is a number of trees in a plot, DBH_{i} is the diameter at breast height of tree i in a sampling plot (m), $\pi \left(\frac{DBH_{\mathrm{i}}}{2}\right)^2$ is the circle basal area of tree i (m^2), $\left(\frac{10^4}{A_{\mathrm{i}}}\right)$ are the scaling factors employed to convert the sampled subplot area (A_{i}) to one hectare (unitless). The *BA* for each land-cover class was represented by the mean *BA* of all plots within a class.

We calculated the mean and standard deviation of *DBH* and *H* for each plot and land cover. We further used these for establishing relationships between *DBH* and *H*, as such relationships serve as functional traits characterizing tree growth patterns and successional stages within forest communities (Nyirambangutse et al., 2017; Howell et al., 2022). We used natural logarithms and then converted them to power-law relationships both plot- and land-cover class-wise (West and Brown, 2005). An ordinary least-square linear regression (OLS) was applied to investigate the *DBH-H* relationship, followed by transforming the relationship into a power-law relationship (Huxley, 1932).

$$H = K_1 DBH^{K_2} \tag{6}$$

Where K_1 and K_2 are the power-law intercept and slope, respectively. The K_1 captures the overall scaling relationship between *H* (m) relative to *DBH* (cm) within a forest community while K_2 regulates the rate of *H* increase relative to *DBH* growth.

The obtained K_1 and K_2 values were further used to estimate *AGB* (AGB_{h}) Eq. (7) in Table 2. We also computed the *AGB* using existing equations (Table 2, Eqs. (9–11)) (AGB_{f}) adopted for the three different land-cover classes. These EF and RF allometric equations were developed for tropical multiple species, whereas the CP was a species-specific allometric equation for the cashew tree (Malimbwi et al., 2016). The wood density values required for the *AGB* estimations were species-specific and obtained from The International Council for Research in Agroforestry (2022) and Zanne et al. (2009). When multiple *WD* values for a tree species were available, the mean value was used, whereas when no species-specific *WD* values were available, the average of tropical Asia (0.57 g cm^{-3}) was used (Reyes et al., 1992). The applied *WD* values for this study then ranged from 0.39–1.04 g cm^{-3}. Specifically, the *WD* values (mean ± a standard deviation) for EF, RF, and CP were 0.74 ± 0.17 g cm^{-3}, 0.72 ± 0.15 g cm^{-3}, and 0.45 g cm^{-3}, respectively. We first estimated *AGB* at the plot level in kilograms, then scaled these values to megagrams per hectare, and averaged per land-cover class.

Table 2. Allometric equations used for estimating aboveground biomass (*AGB*, kg tree^{-1}) in the different land-cover classes.

No.	Equations	Land cover	*AGB* allometric equations	Regions	n	*DBH* (range, cm)	$\overline{WD}_{\mathrm{f}}$ (mean ± SD, g cm^{-3})	References
1	Eq. (7)	All	$AGB_{\mathrm{h}} = \frac{WD\ \pi\ K_1}{8}\ DBH^{2+K_2} + \varepsilon$	-	-	-	-	This study
2	Eq. (8)	All	$AGB_{\mathrm{wd}} = \frac{WD}{\overline{WD}_{\mathrm{f}}}\ AGB_{\mathrm{f}}$	-	-	-	-	This study
3	Eq. (9)	EF	$AGB_{\mathrm{f}} = 0.1184\ DBH^{2.53}$	Pantropical	170	5.0–148.0	0.58 ± 0.02	Brown (1997)
4	Eq. (10)	RF	$AGB_{\mathrm{f}} = 0.0829\ DBH^{2.43}$	Sarawak, Malaysia	136	0.1–28.7	0.38 ± 0.07	Kenzo et al. (2009)
5	Eq. (11)	CP	$AGB_{\mathrm{f}} = 0.8450\ DBH^{1.77}$	Pwani, Tanzania	45	6.0–89.9	0.18	Malimbwi et al. (2016), Mlagalila (2016)

Note: EF is evergreen forests, RF is regrowth forests, CP is cashew plantations. In Eqs. (9–11), *DBH* is diameter at breast height (cm), and $\overline{WD}_{\mathrm{f}}$ is the reported mean wood density used in AGB_f (kg m^{-3}). In Eq. (7), K_1 and K_2 are derived power-law intercept and slope values between *DBH* (cm) and tree height (*H*, m) relationship in Eq. (6), ε is a statistical error term, *WD* is wood density for each tree species (g cm^{-3}), and *DBH* is in centimetres. In this study, in Eq. (7), we employed a trunk shape factor of 1/8 for calculating the volume of frustum cones, as proposed by King et al. (2006). This factor falls within the range of 1/4 (cylinder volumes) to 1/12 (cone volumes). In Eq. (8), AGB_{wd} is our examined aboveground biomass based on equations Eqs. (9–11) with species-specific wood density updated for our woody tree species, WD are the species-specific wood density of trees in each plot (g cm^{-3}).

2.3.4 Statistical analysis

Descriptive statistics were conducted to examine the difference in ecosystem characteristics between plots and land-cover classes. One-way ANOVA tests (ANOVA) were used to assess significant differences in mean values across land-cover classes. Tukey's Honestly Significant Difference test (Tukey HSD) was further employed for pairwise comparisons between land-cover classes. Pearson correlation and ordinary least squares regression analyses were used to explore relationships between variables. All analyses were performed using R 4.2.3 (R Core Team, 2023).

3 Results

3.1 Meteorological and soil conditions

The observed annual daily mean air temperature from April 2022 to April 2023 at Kulen meteorological station was 24.2 ± 2.0 °C, varying between 17.8 °C and 28.6 °C (Fig. 2a). The total annual rainfall was 2290 mm, significantly surpassing nearby lowland stations: Banteay Srei station, located 22 km west, recorded 1160 mm, and Siem Reap City station, situated 40 km southwest, recorded 1475 mm (Chim et al., 2021). About 90 % of the annual precipitation fell during the rainy season from May to November, with September being the wettest month (505 mm). The daily maximum rainfall can reach up to 141 mm, but the daily mean during the rainy season was 11.2 ± 19.7 mm (Fig. 2b). The annual daily mean of global radiation, relative humidity, vapour pressure deficit, and wind speed were 172 ± 44 W m^{-2}, 88 ± 12 %, 0.45 ± 0.21 kPa, and 0.68 ± 0.22 m s^{-1}, respectively (Fig. 2c–f).

Soil conditions varied significantly among land-cover classes (ANOVA and Tukey HSD, p-value < 0.001). Annual daily mean soil temperature was highest in CP (25.8 °C), exceeding values in EF (24.3 °C) and RF (24.2 °C). In contrast, annual daily mean soil water content was lowest in RF (0.14 m^3 m^{-3}) compared to EF (0.23 m^3 m^{-3}) and CP (0.21 m^3 m^{-3}) (Table 3). Annual daily mean soil electrical conductivity was highest in EF (0.039 dS m^{-1}), followed by RF (0.032 dS m^{-1}) and CP (0.025 dS m^{-1}). Overall, daily mean values across land-cover classes ranged between 0.14–0.23 m^3 m^{-3} for *SWC*, 24.2–25.8 °C for *Ts*, and 0.025–0.039 dS m^{-1} for *ECs* (measured at 20 cm depth, Fig. 2g–i).

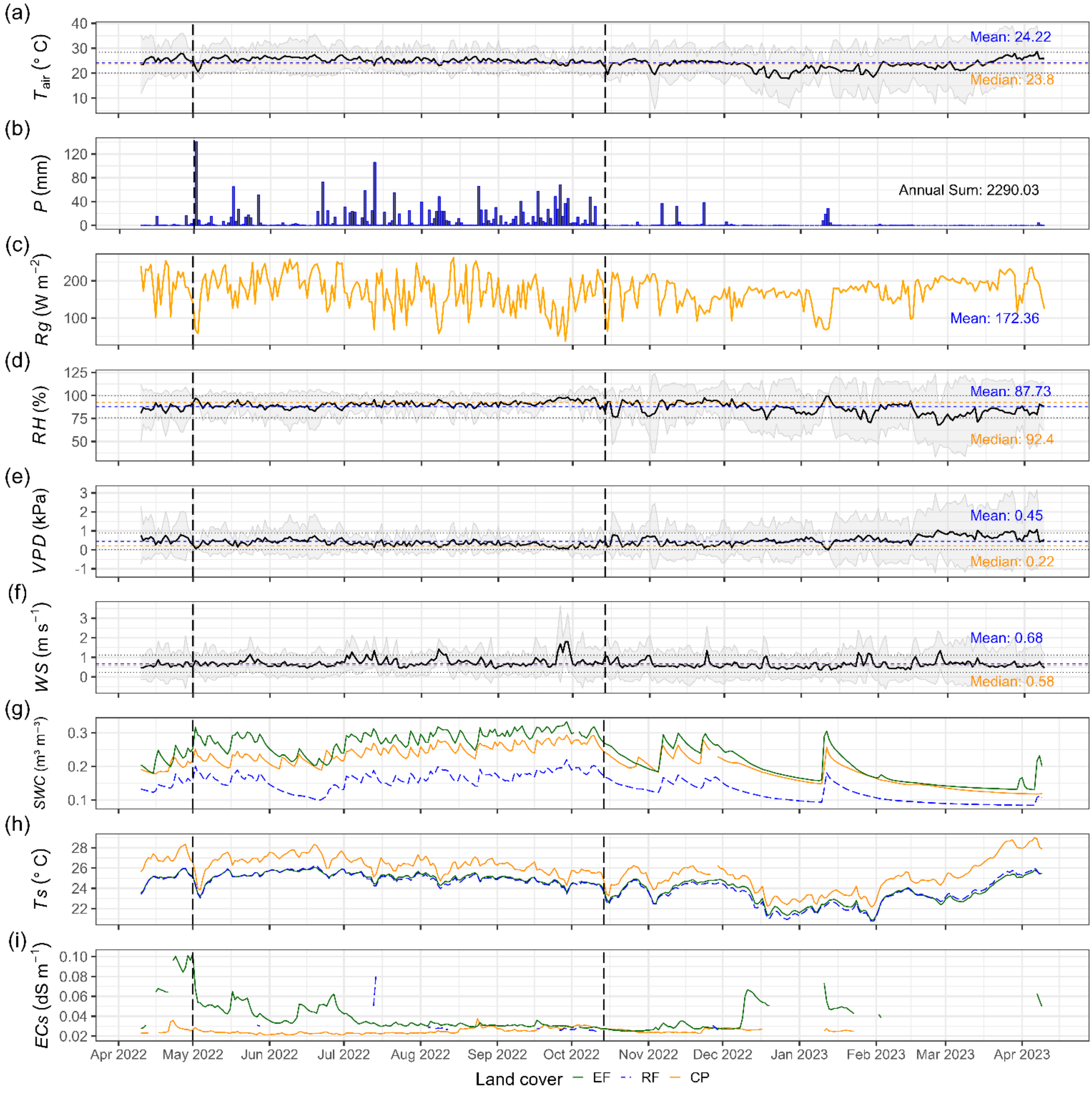

Figure 2. The meteorological conditions at Kulen meteorological station (a–f), and soil conditions at each land-cover class (g–i) from April 10, 2022, to April 9, 2023. (a) Daily mean air temperature (T_{air}, °C), (b) daily total precipitation (P, mm), (c) daily mean global radiation (Rg, W m^{-2}), (d) daily mean relative humidity (RH, %), (e) daily mean vapour pressure deficit (VPD, kPa), and (f) daily mean wind speed (WS, m s^{-1}), (g) daily mean soil water content (SWC, m^3 m^{-3}), (h) daily mean soil temperature (Ts, °C), (i) daily mean soil saturation extraction electrical conductivity (ECs, dS m^{-1}). The vertical dashed line region in all the plots highlighted the rainy season period in Cambodia from May to October. The grey-shaded regions around the mean in (a), (d), (e), and (f) represent the 95 % confidence interval (using a standard deviation) from the daily mean, whereas the blue horizontal dashed line represents

the yearly mean, the brown horizontal dashed line represents the yearly median, and the black horizontal dotted line represents a yearly standard deviation (see Table S2.1 and Fig. S2.2 present the Kulen meteorological station's annual and monthly meteorological data. Figs. S3.1–S3.3 shows monthly mean soil conditions by land-cover class, and Fig. S4.1 depicts correlations between meteorological and soil conditions).

3.2 Species diversity

A total of 343 observations (292 trees and 51 seedlings) from 47 woody species (including 13 seedling species) and 32 families (including seven seedling families) were identified from the nine plots (Table S5.1). No statistical test of significance of differences in species diversity among land cover classes was possible due to too few sampled plots. However, species diversity declined markedly from evergreen forests to regrowth forests and was lowest in cashew plantations, as reflected in both species richness and in the Shannon-Wiener index. The average S_R per plot was 17 in EF, 13 in RF, and only 4 in CP. Similarly, the S_H was highest in EF (2.48 ± 0.33), intermediate in RF (1.97 ± 0.45), and lowest in CP (0.61 ± 0.46), with individual plot values ranging from 0.31 (CP2) to 2.68 (EF1) (Table S5.2). Species composition was more evenly distributed in EF and RF, but naturally strongly dominated by a single species in CP. In EF, the top five most abundant species, *Mesua ferrea* (n = 18), *Diospyros bejaudii* (n = 12), *Litchi chinensis* (n = 11), *Vatica odorata* (n = 11), and *Hydnocarpus annamensis* (n = 8), accounted for 46 % of the individuals. In RF, *Vatica odorata* (n = 54), *Nephelium hypoleucum* (n = 14), *Benkara fasciculata* (n = 12), *Garcinia oliveri* (n = 12), and *Mesua ferrea* (n = 5) made up 61 %. In contrast, CP was dominated by *Anacardium occidentale* (n = 46), which was the only tree species observed excluding seedlings. Additional seedling species in CP included *Strychnos axillaris* (n = 3), *Nephelium hypoleucum* (n = 1), *Melodorum fruticosum* (n = 1), *Maclura cochinchinensis* (n = 1), and *Catunaregam tomentosa* (n = 1). Furthermore, fast-growth species, as described by Ha (2015) ($WD < 0.6$ g cm^{-3}), accounted for 40 % of EF and 44 % of RF of their total species composition.

Table 3. Mean values and statistics of ecosystem characteristics in the different land-cover classes.

Group	Variables	Land cover						ANOVA	Tukey HSD		
									CP & EF	RF & EF	RF & CP
		EF (Mean ± SD)	n	RF (Mean ± SD)	n	CP (Mean ± SD)	n	p-value	p-value	p-value	p-value
Species diversity	S_R (with seedling species, count per plot)	17 ± 4	3	13 ± 2	3	4 ± 3	3	-	-	-	-
	S_R (without seedling species, count per plot)	13 ± 2	3	10 ± 3	3	1 ± 0	3	-	-	-	-
	S_H (with seedling species, unitless)	2.48 ± 0.33	3	1.97 ± 0.45	3	0.61 ± 0.46	3	-	-	-	-

Leaf functional traits	Chl_{cwm} (mg g^{-1})	9.14 ± 3.45	109	7.56 ± 2.03	137	4.99 ± 0.66	46	*	*	0.39	0.08
	$LDMC_{cwm}$ (mg g^{-1})	398.43 ± 72.24	109	370.13 ± 94.97	137	407.64 ± 21.68	46	0.51	0.50	0.94	0.69
	SLA_{cwm} (m^2 kg^{-1})	18.18 ± 2.86	109	14.87 ± 2.06	137	11.99 ± 1.45	46	**	**	*	0.06
Stand structure	*DBH* (cm)	18.0 ± 20.1	109	5.8 ± 4.3	137	13.0 ± 3.9	46	***	0.14	***	***
	H (m)	17.0 ± 13.3	109	7.4 ± 3.8	137	6.3 ± 1.0	46	***	***	***	0.93
	Maximum *H* (m)	52.0	109	18.6	137	7.8	46	-	-	-	-
	Wood density (g cm^{-3})†	0.74 ± 0.17	109	0.72 ± 0.15	137	0.45 ± 0.00	46	***	***	0.56	***
	Stem density *DBH* > 1 cm (ha^{-1})††	6216 ± 2177	3	10859 ± 4999	3	1067 ± 440	3	-	-	-	-
	Stem density *DBH* > 5 cm (ha^{-1})††	1016 ± 533	3	2193 ± 895	3	1067 ± 440	3	-	-	-	-
	Stem density *DBH* ≥ 10 cm (ha^{-1})††	550 ± 505	3	293 ± 6	3	600 ± 164	3	-	-	-	-
	BA (m^2 ha^{-1})	26.2 ± 3.6	3	17.0 ± 5.4	3	11.6 ± 3.5	3	-	-	-	-
	BA (m^2 ha^{-1}, *DBH* ≥ 5 cm)	23.7 ± 4.4	3	11.6 ± 2.4	3	11.6 ± 3.5	3	-	-	-	-
	BA (m^2 ha^{-1}, *DBH* ≥ 10 cm)	21.1 ± 4.4	3	4.4 ± 0.7	3	9.2 ± 1.8	3	-	-	-	-
	DWB (Total) (Mg ha^{-1})	27.5 ± 12.4	3	4.8 ± 7.0	3	0.4 ± 0.2	3	-	-	-	-
	AGB_f (Mg ha^{-1})	239 ± 92	3	42 ± 10	3	71 ± 22	3	-	-	-	-
	AGB_{wd} (Mg ha^{-1})	336 ± 168	3	78 ± 25	3	182 ± 57	3	-	-	-	-
	AGB_h (Mg ha^{-1})	312 ± 184	3	54 ± 14	3	17 ± 5	3	-	-	-	-
	LAI_C (m^2 m^{-2})	4.62 ± 0.50	21	4.66 ± 0.70	21	2.52 ± 0.42	21	***	***	1.00	***
	LAI_T (m^2 m^{-2})	6.16 ± 0.67	21	5.57 ± 0.76	21	3.07 ± 0.61	21	***	***	0.08	***
	Annual mean *fPAR*‡	0.97 ± 0.01	364	0.96 ± 0.01	365	0.76 ± 0.06	359	***	***	*	***
Soil conditions	Annual mean *SWC*‡ (m^3 m^{-3})	0.23 ± 0.06	364	0.14 ± 0.03	365	0.21 ± 0.05	363	***	***	***	***
	Annual mean *Ts*‡ (°C)	24.3 ± 1.2	364	24.2 ± 1.3	365	25.8 ± 1.5	363	***	***	***	***
	Annual mean *ECs*‡ (dS m^{-1})	0.039 ± 0.015	268	0.032 ± 0.013	40	0.025 ± 0.003	260	***	***	***	***

Note: Abbreviations used in the table: EF = evergreen forests, RF = regrowth forests, CP = cashew plantations, S_R = species richness (only woody seedling species), S_H = Shannon-Wiener index, Chl_{cwm} = community-weighted mean of chlorophyll a and b content, $LDMC_{cwm}$ = community-weighted mean of leaf dry matter content, SLA_{cwm} = community-weighted mean of specific leaf area, *DBH* = tree's diameter at breast height, *H* = tree height, *BA* = stand basal area, AGB_f = aboveground biomass computed by adopted functions, AGB_h = aboveground biomass computed by *H* and *DBH* power-law relationship, AGB_{wd} = aboveground biomass based on equations Eqs. (9–11) with species-specific wood density updated for our woody tree species, LAI_C = canopy leaf area index, LAI_T = total leaf area index, *fPAR* = fraction of photosynthetically active radiation, *SWC* = soil water content, *Ts* = soil temperature, *ECs* = soil saturation extract electrical conductivity, SD = a standard deviation, ANOVA = one-way analysis of variance, Tukey HSD = Tukey's Honestly Significant Difference test. Statistically significant code for ANOVA and Tukey HSD test: '*' p-value < 0.001, '**' p-value < 0.01, '*' p-value < 0.05, and "-" not available. †The species-specific wood density was derived from the ICRAF Database (2022) and Zanne et al. (2009). ††Extrapolated values for one hectare were obtained from sampling *DBH* class subplots. ‡Daily mean values were used to calculate the reported variables.**

3.3 Leaf functional traits

At the species level, the mean specific leaf area for all 30 species was 16.97 ± 5.30 m^2 kg^{-1}, with *Hydnocarpus annamensis* having the highest *SLA* (36.67 ± 5.20 m^2 kg^{-1}) and *Capparis micracantha* the lowest (10.46 ± 3.28 m^2 kg^{-1}). For *Chl*, the mean value was 10.28 ± 4.17 mg g^{-1}, with *Hydnocarpus annamensis* having the highest value (25.75 ± 5.28 mg g^{-1}) and *Anacardium occidentale* the lowest (4.86 ± 4.93 mg g^{-1}). Finally, for *LDMC* the mean value was 378.96 ± 143.26 mg g^{-1}, with *Mesua ferrea* and *Hydnocarpus annamensis* having the highest (486.90 ± 25.03 mg g^{-1}) and lowest (139.92 ± 20.19 mg g^{-1}) values, respectively. For detailed descriptions of leaf functional traits of all species and plots, please refer to Tables S6.1–S6.3.

Across land-cover classes, mean SLA_{cwm} and Chl_{cwm} decreased from EF to RF to CP. SLA_{cwm} and Chl_{cwm} were highest in EF (18.18 ± 2.86 m^2 kg^{-1} and 9.14 ± 3.45 mg g^{-1}) followed by RF (14.87 ± 2.06 m^2 kg^{-1} and 7.56 ± 2.03 mg g^{-1}) and CP (11.99 ± 1.45 m^2 kg^{-1} and 4.99 ± 0.66 mg g^{-1}). Both traits showed statistically significant differences across land covers (ANOVA p-value < 0.002 for SLA_{cwm}, p-value < 0.018 for Chl_{cwm}). In contrast, $LDMC_{cwm}$ did not differ substantially among land-cover classes (p-value = 0.51), with CP having the highest value (407.64 ± 21.68 mg g^{-1}), followed by EF (398.43 ± 72.24 mg g^{-1}) and RF (370.13 ± 94.97 mg g^{-1}). See Table S6.4 for data sources and shared percentages of species trait values used to compute SLA_{cwm}, Chl_{cwm}, and $LDMC_{cwm}$.

3.4 Stand structure attributes

DBH and tree height

Land-cover conversion reduces both the mean and variability of tree diameter and height, indicating a loss of structural complexity in human-disturbed ecosystems. Structural measurements of 292 woody trees across three land-cover classes showed that EF had the highest structural complexity, with the highest mean and variability in *DBH* (18.0 ± 20.1 cm) and tree height (17.0 ± 13.3 m), including the largest individuals (*DBH* = 102.3 cm, *H* = 52.0 m, Fig. S7.1). However, RF and CP had substantially lower means and variability in these variables, suggesting reduced structural complexity after forest conversion. While both RF and CP had similar heights (RF: 7.4 ± 3.8 m, CP: 6.3 ± 1.0 m), CP had a significantly greater *DBH* (CP: 13.0 ± 3.9 cm, RF: 5.8 ± 4.3 cm). The results of the ANOVA and Tukey HSD tests confirmed significant differences in *DBH* and height among land covers (p-value < 0.001), except for CP and EF for *DBH* and CP and RF for height (Table 3).

Aboveground and deadwood biomass

Land-cover conversion from EF to RF and CP resulted in a substantial decline in both aboveground and deadwood biomass. The mean AGB_f estimated using the generic allometric function dropped sharply from 239 ± 92 Mg ha^{-1} in EF to 42 ± 10 Mg ha^{-1} in RF and 71 ± 22 Mg ha^{-1} in CP. Similarly, the mean total *DWB* declined from 27.5 ± 12.4 Mg ha^{-1} in EF, 4.8 ± 7.0 Mg ha^{-1} in RF, and 0.4 ± 0.2 Mg ha^{-1} in CP. See Table A1 for the contribution of lying and standing *DWB* to total *DWB*.

Stem density and basal area

Changes in land cover strongly influenced stem density, basal area, and the distribution of aboveground biomass across *DBH* classes (Fig. 3). RF exhibited twice the stem density (*DBH* > 5 cm) per hectare compared to EF and CP, driven largely by a high proportion of smaller trees in the 5–15 cm *DBH* class. Despite having a lower mean *DBH*, RF had a higher basal area (17.0 ± 5.4 $m^2\ ha^{-1}$) than CP (11.6 ± 3.5 $m^2\ ha^{-1}$). Interestingly, in EF, only 5 % of the stems with a *DBH* > 30 cm contributed to approximately 65 % of the total AGB_f. In contrast, the main *DBH* class contributing to the AGB_f in RF and CP was 5–15 cm, accounting for 57 % and 76 % of the total AGB_f in RF and in CP, respectively. Refer to Supplementary Table S7.1 for shared stem density percentages per hectare across *DBH* classes, and Table S7.2 for shared percentages of AGB_f categorized by *DBH* class.

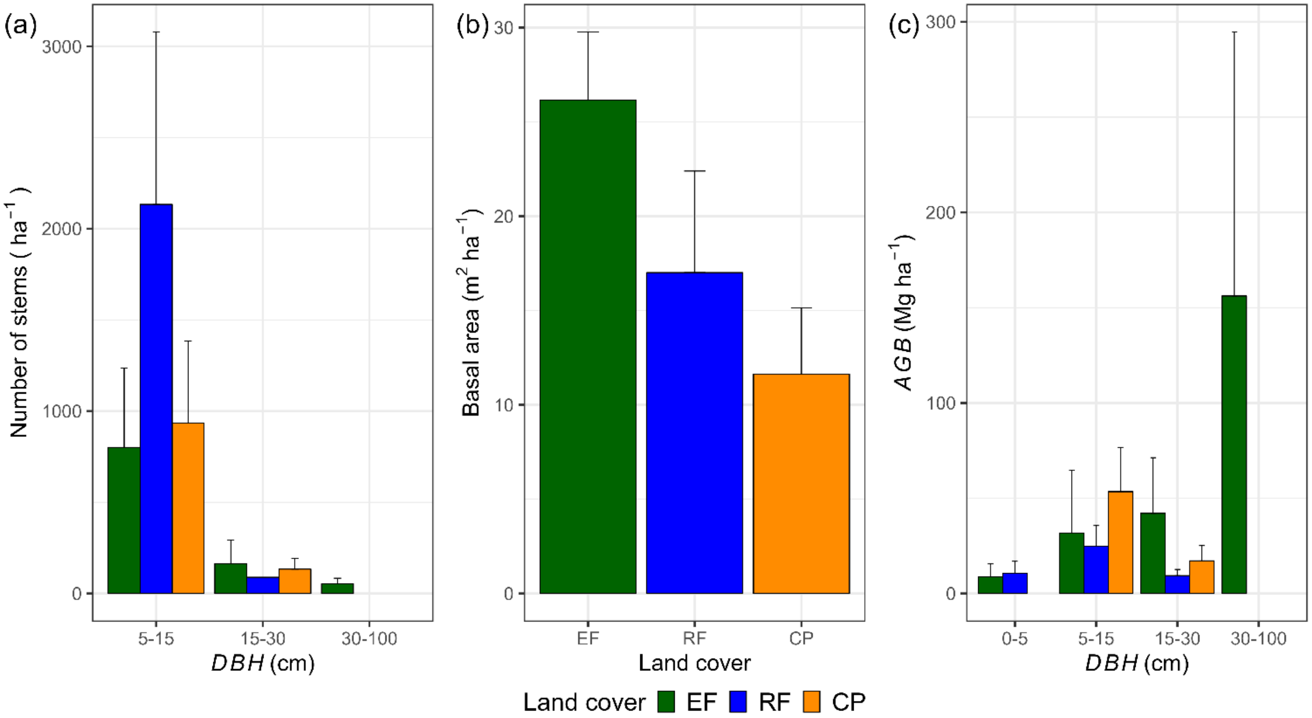

Figure 3. Estimations per land-cover class of a mean number of stems per hectare (a), basal area (*BA*, $m^2\ ha^{-1}$) (b), and mean aboveground biomass separated by the different diameters at breast height (*DBH*) classes (c). In (c), the contribution of different *DBH* classes to the mean aboveground biomass estimated by the AGB_f method was used in this calculation. The error bars in the figure represent one standard deviation.

LAI and *fPAR*

The mean total leaf area index values were 6.16 ± 0.67 $m^2\ m^{-2}$ for EF, 5.57 ± 0.76 $m^2\ m^{-2}$ for RF, and 3.07 ± 0.61 $m^2\ m^{-2}$ for CP. The mean canopy *LAI* values were 4.62 ± 0.5 $m^2\ m^{-2}$ for EF, 4.66 ± 0.70 $m^2\ m^{-2}$ for RF, and 2.52 ± 0.42 $m^2\ m^{-2}$ for CP. The ANOVA analysis revealed a significant difference in mean LAI_T and mean LAI_C among the three land-cover classes, while the Tukey HSD test did not find a significant difference in mean LAI_T and mean LAI_C between EF and RF (Table 3). The phenology of both LAI_{T} and LAI_{C} revealed a similar pattern in EF and RF, with peak and base values in June and March, respectively (Fig. 4a–b, Table S7.3). The LAI_{T} and LAI_{C} patterns for CP resembled those of EF and RF but also had a strong decrease in April. Furthermore, the understory *LAI* (LAI_{U}; the difference between LAI_{T} and LAI_{C}) for the various land-cover classes indicates that the ground vegetation highly contributes to LAI_{T} for EF and RF, while the contribution was minor for CP (Fig. 4c). In particular, the LAI_{U} mean values within a year were approximately 1.54 ± 0.57 $m^2\ m^{-2}$ for EF (25 %), 0.91 ± 0.36 $m^2\ m^{-2}$ for RF (16 %), and 0.55 ± 0.39 $m^2\ m^{-2}$ for CP (18 %). A general trend of high contribution LAI_{U} to LAI_{T} in June and low contribution in April was apparent for all land-cover classes.

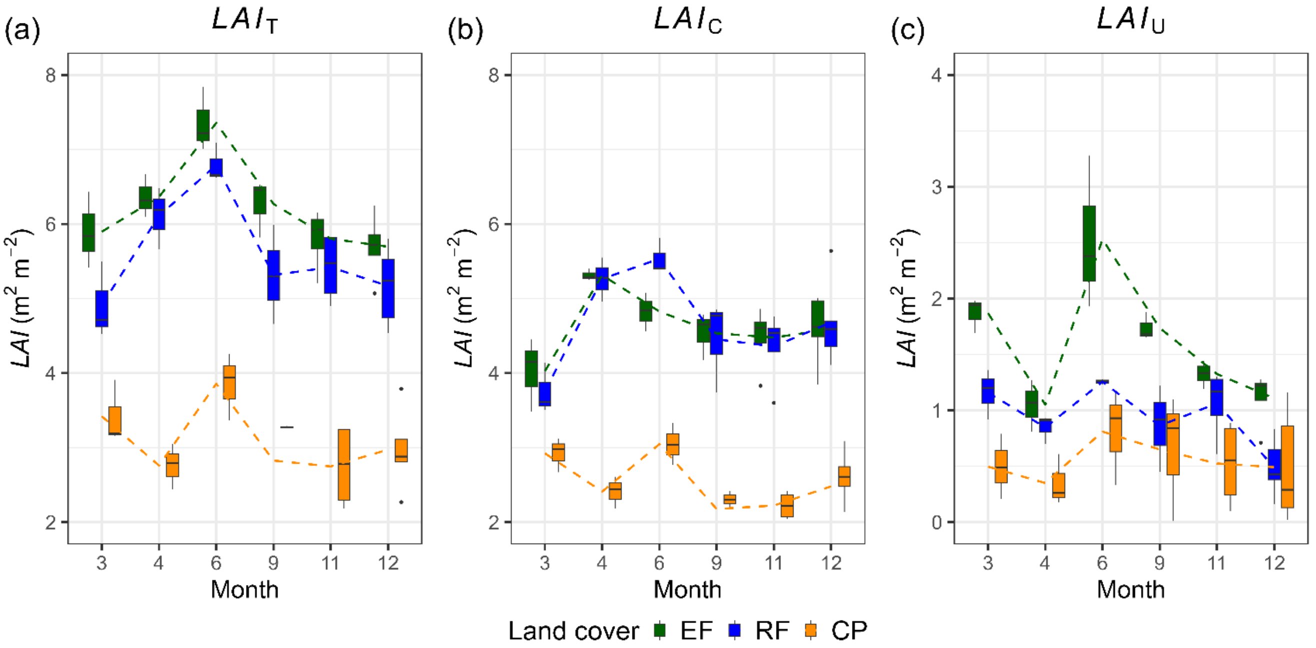

Figure 4. Total leaf area index (LAI_{T}, $m^2\ m^{-2}$), canopy leaf area index (LAI_{C}, $m^2\ m^{-2}$), and understory leaf area index (LAI_{U}, $m^2\ m^{-2}$), their variations across different months within a year for evergreen forests (EF), regrowth forests (RF), and cashew plantations (CP). The lines in the graph represent the connection between the mean *LAI* values from one month to another.

The observed mean annual *fPAR* for EF, RF, and CP was high: 0.97 ± 0.01, 0.96 ± 0.01, and 0.76 ± 0.06, respectively (Table 3). The values of EF and RF exhibited minimal fluctuations throughout the year, whereas the *fPAR* of CP ranged between 0.55 and 0.93 (Fig. 5). Like *LAI*, the annual mean *fPAR* among EF, RF, and CP were statistically significantly different according to both the ANOVA test and Tukey HSD’s tests.

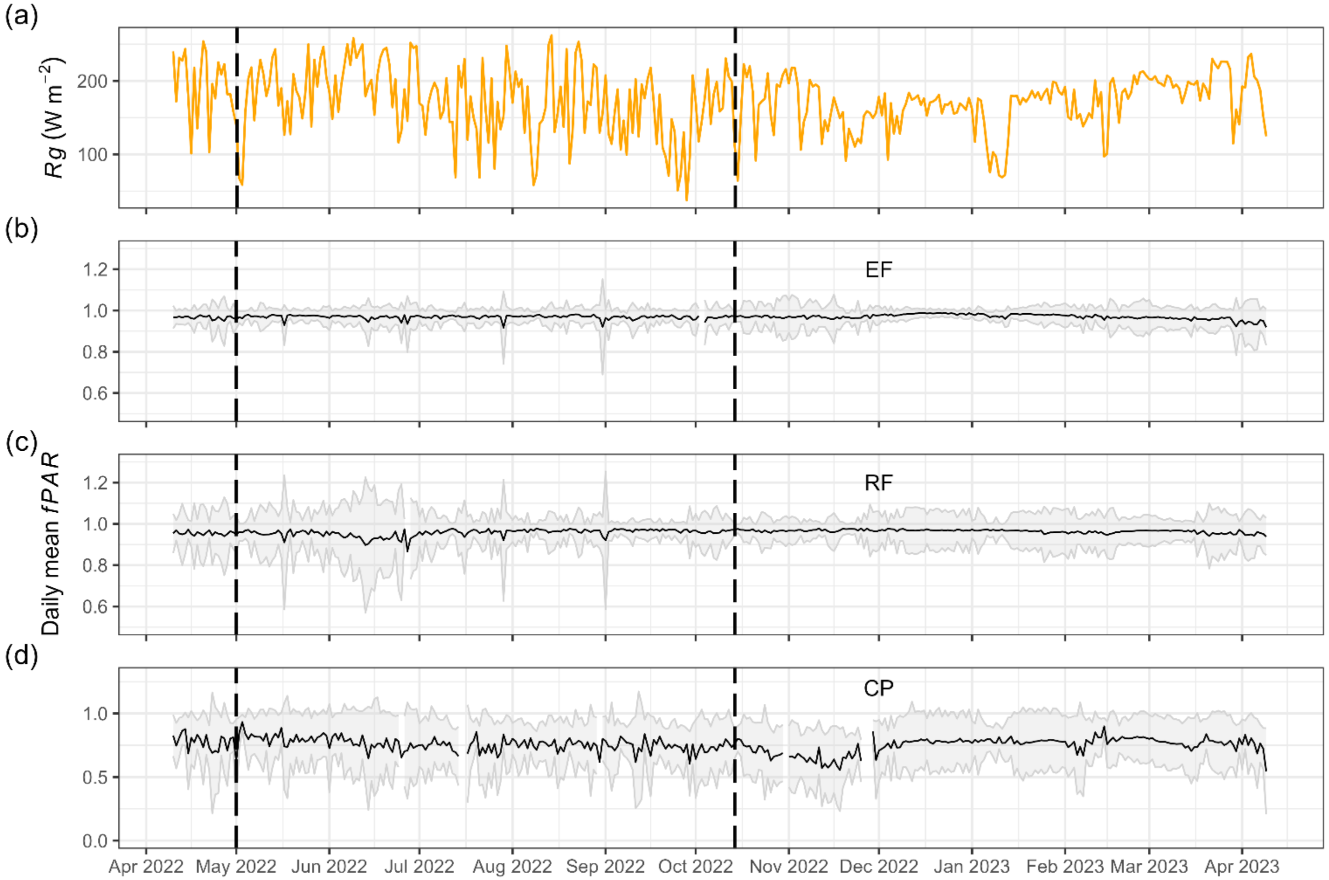

Figure 5. Daily mean global radiation (*Rg*, W m^{-2}) (a) and daily mean *fPAR* for evergreen forests (EF) (b), regrowth forests (RF) (c), cashew plantations (CP) (d) from April 11, 2022, to April 9, 2023 at Kulen. The shaded area represents one standard deviation from the mean, computed using the ten *PAR* sensors installed in each land-cover class.

3.5 Estimated Aboveground biomass based on *DBH-H* relationship

DBH-H relationship

Land-cover change weakens tree allometry, reducing the consistency of *DBH-H* relationships in human-impact forest and agricultural ecosystems. Strong positive relationships between *DBH* and *H* were observed in both EF and RF. For EF, 92 % of the variation in *H* can be explained by the variation in *DBH*, whereas for RF and CP, it was 78 % and 51 %, respectively (Fig. 6, Table S7.4). The power-law relationships between *DBH* and *H* further indicated that the K_1 and K_2 values for EF and RF were similar, whereas the values for CP were much lower. For a plot-level analysis of relationships between ln(*DBH*) and ln(*H*), see Fig. S7.2 and Table S7.5.

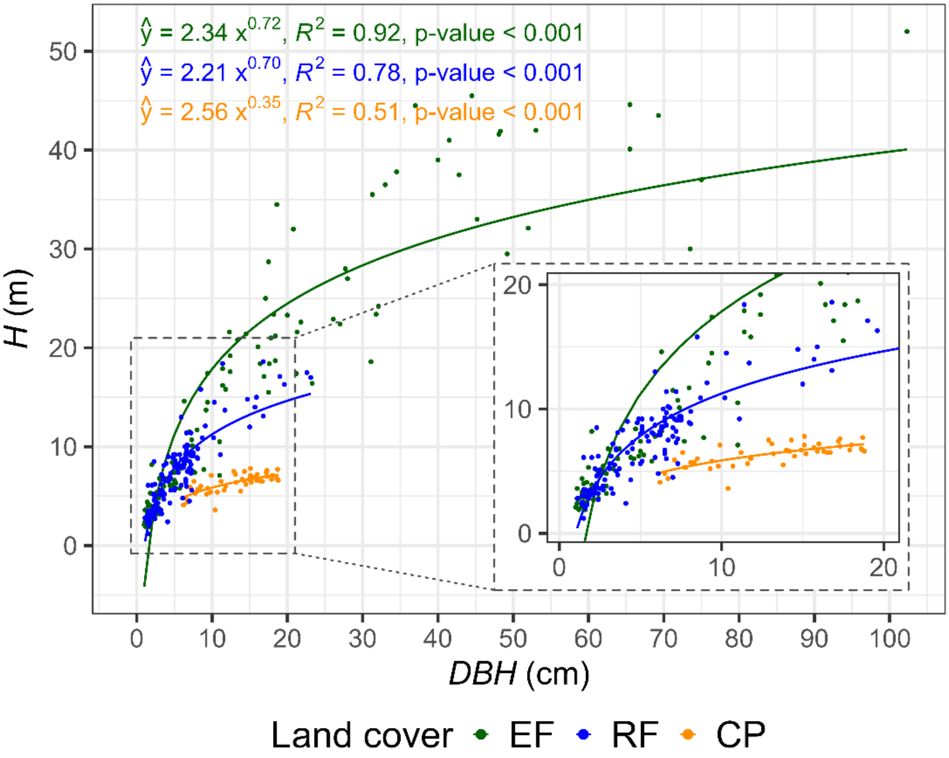

Figure 6. Relationship between diameter at breast height (*DBH*) (cm) and tree height (*H*) (m) for evergreen forests (EF), regrowth forests (RF), and cashew plantations (CP) in Kulen. Figure shows the derived power-law intercept (K_1) and slope (K_2) values for EF, RF, and CP.

Comparison of *AGB* estimation methods

Our results indicate that locally calibrated *DBH-H* relationships and species-specific wood density substantially affected aboveground biomass estimates compared to generalized models (Fig. 7). The AGB_{wd} method consistently produced higher values than AGB_f across all land-cover classes, reflecting the influence of wood density and the dominance of high-density tree species at our study site. In EF and RF, where *DBH-H* relationships were strong, AGB_h estimates were markedly higher than AGB_f (EF: 239 ± 92 vs. 312 ± 184 Mg ha^{-1}, RF: 42 ± 10 vs. 54 ± 14 Mg ha^{-1}), consistent with plot-level regression results (Fig. S7.2, Table S7.5). In contrast, in CP, AGB_h yielded much lower values than AGB_f (17 ± 5 vs. 71 ± 22 Mg ha^{-1}), highlighting the limited reliability of this method under weak *DBH-H* relationship conditions. The differences between AGB_h and AGB_f estimates across land covers are illustrated in 1:1 comparison plots and plot-level summaries (Figs. S7.3–S7.5).

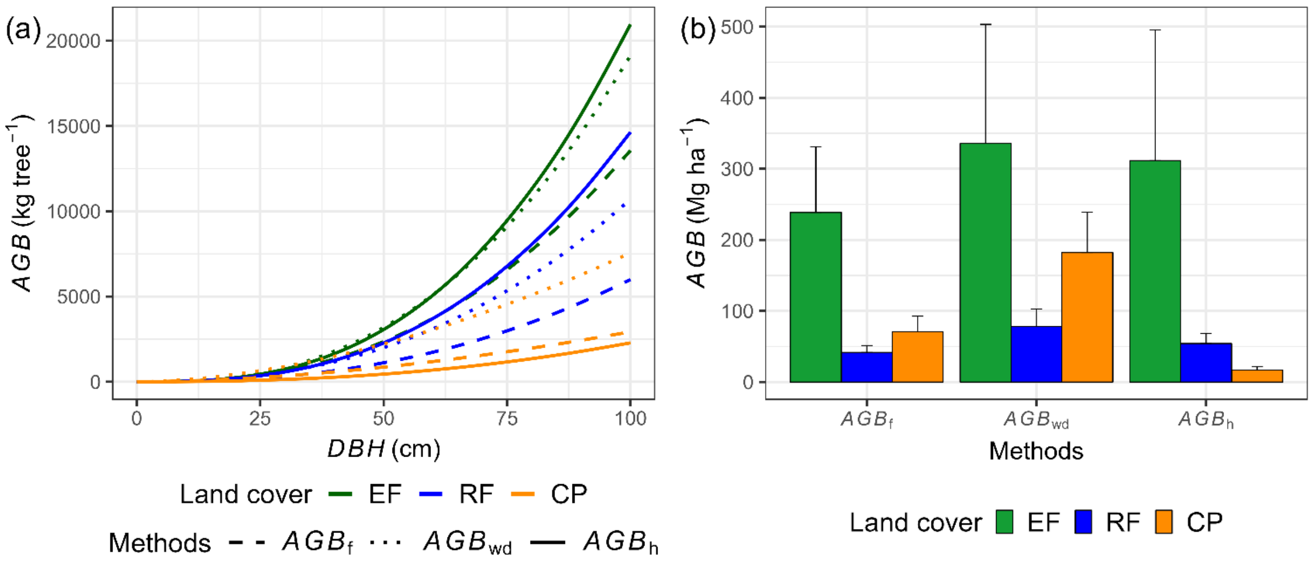

Figure 7. Power-law relationships between aboveground biomass (*AGB*) of *AGB*$_f$, *AGB*$_h$, and *AGB*$_{wd}$ and diameter at breast height (*DBH*) for each land-cover class (a), along with the corresponding results of *AGB* estimation (b). *AGB*$_f$ represents aboveground biomass estimated by adopted functions, *AGB*$_{wd}$ represents aboveground biomass estimated by adopted functions utilizing species-specific wood density, and *AGB*$_h$ represents aboveground biomass estimated by the *DBH* and tree height (*H*) relationship, in conjunction with species-specific wood density, for the study site. The error bar in (b) represents a standard deviation.

3.6 *AGB*$_h$ relationships with *LAI*$_T$, *SLA*$_{cwm}$, and *S*$_R$

We observed positive relationships between aboveground biomass and three pivotal ecosystem characteristics: *LAI*$_T$, *S*$_R$, and *SLA*$_{cwm}$ determining 76 %, 72 %, and 68 % of the variability in *AGB*, respectively (Fig. 8, Table S8.1 for statistical regression tables). *LAI*$_T$ exhibited strong positive correlations with *SLA*$_{cwm}$, *S*$_R$, and *AGB*, with the Pearson correlation coefficient in the range of 0.67–0.85. *SLA*$_{cwm}$ had a positive correlation with *S*$_R$ and *AGB*. Furthermore, additional insights regarding the Pearson correlation matrix depicting relationships among various ecosystem characteristics are presented in Fig. S8.1.

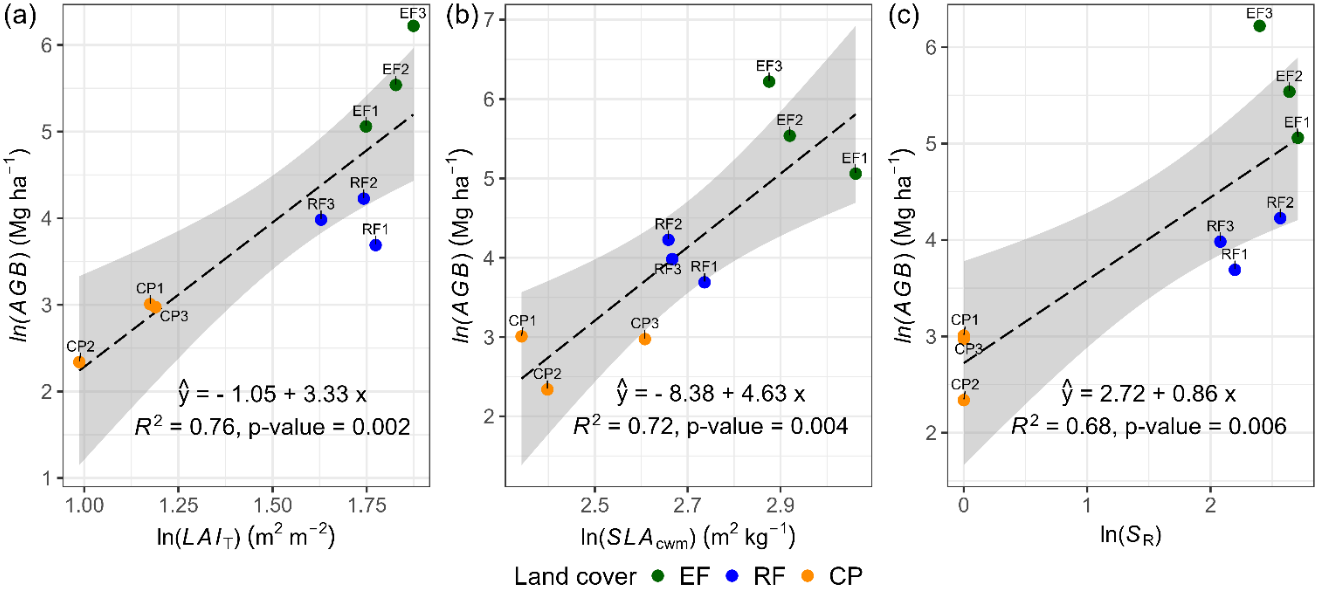

Figure 8. Ordinary least squares regression showing the effect of mean total *LAI* (*LAI_T*, m^2 m^{-2}), mean *SLA_{cwm}* (m^2 kg^{-1}), and species richness (*S_R*, count per plot) on *AGB*. Mean *LAI_T* is a mean ground *LAI* measurement, *S_R* is a woody species count excluding seedlings in a plot, and *AGB* is *AGB_h* whose estimation was based on the *DBH-H* relationship.

4 Discussions

4.1 Soil conditions

The observations of soil temperature, soil water content and soil electrical conductivity all support our hypothesis that land-cover conversion changes soil conditions in these tropical forest ecosystems. The difference in soil temperature between the forested land-cover classes (EF and RF) and the cashew plantations (Table 3) aligns with prior studies by van Haren et al. (2013) and Geng et al. (2022) and can be explained by the substantial difference in interception of incoming radiation between these ecosystems (Fig. 4). The multi-layered canopies and the dense layer of deadwood and litterfall, effectively prevent direct sunlight from reaching the ground. This natural shield reduces the impact of solar irradiance, thereby maintaining cooler soil surface temperatures (Senior et al., 2018). Conversely, CP has a simpler canopy structure, predominantly featuring a single layer of cashew trees of similar age. The understory in these areas is sparser, and the reduction in deadwood, due to management, facilitates greater penetration of solar irradiance and elevates soil temperatures.

Our observed annual mean soil water content across the three land-cover classes (0.14–0.23 m^3 m^{-3}) is consistent with earlier findings (Rodell et al., 2004; Wang et al., 2012; Horel et al., 2022). Variations in *SWC* among these classes may stem from differences in their stand structural complexity (vegetation cover and root system) and soil properties (organic matter content and texture) (Pickering et al., 2021; Tang et al., 2021). The higher *SWC* in evergreen forests compared to regrowth forests is attributed to their dense and multilayered vegetation cover, which reduces penetration of solar irradiance and temperature at the forest floor, thereby reducing evaporation and maintaining topsoil moisture (Fig. 4). In addition, the complex root systems of primary forests enhance water retention by creating channels and pores in the soil, while organic matter from deadwood and litterfall further enhances soil water retention, particularly during arid conditions (Luo et al., 2023). Another explanation could be the soil texture, as our field investigation observed that cashew plantations are all on sandier soils with lower water-holding capacity, leading to decreased *SWC* (Ibrahim and Alghamdi, 2021). Nevertheless, further examination of soil samples is necessary to accurately measure the specific soil properties in each land-cover class.

The analysis of soil electrical conductivity categorized the soils as non-saline across the land-cover classes. Evergreen forests had higher *ECs* than cashew and regrowth forests, potentially indicating larger nutrient availability (Omuto et al., 2020). This higher nutrient availability in evergreen forests may be linked to greater organic matter decomposition, species richness, higher soil moisture content, and no history of being clear-cut, which could lead to nutrient losses via run-off during the phase without vegetation (Austin et al., 2004; Vestin et al., 2020; Guo et al., 2023b).

4.2 Species diversity

Species richness and Shannon-Wiener index clearly declined from evergreen forests to regrowth forests and were lowest in cashew plantations, supporting our hypothesis that land-cover conversion reduces species diversity. While EF and RF showed similar mean values to other evergreen forests in the mainland of Southeast Asia and India (Zin and Mitlöhner, 2020; Theilade et al., 2022; Tynsong et al., 2022), S_R was lower compared to the most diverse rainforests in South America and equatorial Southeast Asia, where often > 250 species ha^{-1} have been reported (Mohd Nazip, 2012; ter Steege et al., 2023) and S_H was lower than for some moist evergreen and humid lowland forests in the region (Mohd Nazip, 2012; Zin and Mitlöhner, 2020). These tropical rainforests may have more species because of their larger forest patch sizes and higher rainfall, compared to the relatively isolated monsoon forest at the top of Kulen, surrounded by agricultural areas (Galanes and Thomlinson, 2009). The relatively low S_H may also be explained by the high proportion of the top five dominant species in each land cover, accounting for over 50 % of total stems in their communities. Another possible reason could be the limited number of sample plots, which may not fully capture the overall species composition and distribution in these forests. Tropical tree species composition is markedly influenced by biogeography and disturbance history, showing significant local variations even over short distances (Whitmore, 1998; Van and Cochard, 2017). This emphasizes the necessity for comprehensive field data sampling to accurately assess the species richness and evenness of these highly diverse plant communities. The comparison between S_R and S_H of EF and RF with previous studies is presented in Table S9.1– S9.2.

4.3 Leaf functional traits

Specific leaf area, leaf dry matter content, and chlorophyll content are all key leaf traits in the leaf economic spectrum, and carry diverse implications for understanding carbon sequestration, resource availability, successional stages, and environmental responses (Wright et al., 2004; Gao et al., 2022). Our results support the hypothesis that changing from pristine evergreen forests to regrowth forests and cashew plantations leads to a substantial decline in key leaf functional traits, particularly specific leaf area and chlorophyll content, indicating reduced ecosystem productivity and resource-use efficiency.

Our observations emphasize the significant consequences of transitioning from EF to RF or CP, resulting in a substantial reduction in actual values and diversity in SLA_{cwm}, reflecting a reduction in both ecosystem productivity and resilience to disturbances (Liu et al., 2023). The higher SLA_{cwm} in EF, suggests higher photosynthetic capacity, especially in shaded environments, due to its dense canopy cover and abundant resource availability (water and nutrients) for plant growth (Green et al., 2020). High SLA_{cwm} values also link to faster turnover and promote nutrient cycles, carbon sequestration, and nutrient use efficiency in forest ecosystems (Guerrieri et al., 2021). The lower SLA_{cwm} values of RF and CP may be attributed to limited water and nutrient availability in the soil because of high competition in those ecosystems. The notable reduction in SLA_{cwm} caused by the shift from EF to RF or CP underlines the profound impact land-cover change has on ecosystem productivity, resilience, and overall functioning. Our SLA_{cwm} of EF exceeded the mean values of tropical forests in Bolivia, Brazil, Costa Rica, and China (Finegan et al., 2015; Wang et al., 2016). The SLA_{cwm} of RF was somewhat higher than the mean of neotropical regrowth forests, but still within the range (Poorter, 2021). SLA_{cwm} in CP was greater than the range value in Parakou, Benin, but fell within the range reported for 15 cashew varieties in Karnataka, India (Akossou et al., 2016; Mog and Nayak, 2018).

Chlorophyll is essential for photosynthesis and serves as a crucial indicator of a plant's photosynthetic capacity, profoundly influencing overall growth (Stirbet et al., 2020). The elevated Chl_{cwm} seen in EF can be attributed to the well-developed and dense canopy structure, which creates a light-shaded environment. This prompts plants to invest more in chlorophyll production, enhancing light harvesting efficiency (Niinemets, 2010). Meanwhile, RF, experiencing intense competition for light in early successional stages, may exhibit lower chlorophyll levels as resources prioritize vertical growth over chlorophyll production (Laurans et al., 2014). Our CP had lower Chl_{cwm} than EF and RF due to less light competition and higher temperatures, which could lead to photoinhibition and lowered leaf chlorophyll content (Rosa et al., 2020). Our Chl_{cwm} of EF and RF falls within the range, but surpasses the mean Chl_{cwm} observed in Chinese forest ecosystems (Li et al., 2018).

Leaf dry matter content is a measure of construction cost per fresh weight mass unit, and it serves as a metric for a plant's resource use strategy and resilience to environmental stresses (Guo et al., 2023a). The higher $LDMC_{\mathrm{cwm}}$ in EF compared to that of RF indicates a conservative resource usage, longer leaf lifespan, and increased carbon sequestration, implying higher ecosystem stability and function for EF (Rawat et al., 2021). Conversely, the highest $LDMC_{\mathrm{cwm}}$ in CP, is attributed to cashew monoculture and the species' high resilience to environmental stress, especially in nutrient-poor soils and water-stressed conditions (Bezerra et al., 2007). This study emphasises EF's increased stress tolerance, conservative resource utilisation and greater carbon sequestration compared to RF, while also emphasizing cashew as a highly proficient species in environmental stress tolerance.

4.4 Stand structure attributes

DBH and tree height

Our findings confirm significant differences in mean *DBH* and tree height resulting from the conversion of pristine evergreen forests to young regrowth forests and cashew plantations following human disturbance. The observed reduction in large-diameter and tall trees in regrowth forests and cashew plantations compared to the evergreen forests (Fig. 3) provides clear evidence of structural degradation, which negatively affects crucial key ecosystem functions such as carbon storage, nutrient cycling, and biodiversity (Díaz et al., 2007; Lutz et al., 2018; Thiel et al., 2021). Observed species in our evergreen forests, such as *Dipterocarpus costatus*, *Sandoricum indicum*, *Mesua ferrea*, *Nageia wallichiana*, and *Litchi chinensis* reach heights of 40–52 m, similar to those found in Cambodia's central evergreen forests (Theilade et al., 2022). Our mean *DBH* of evergreen forests is comparable to mature tropical forests in Vietnam and falls within the pantropical range, while regrowth forests have a slightly higher mean *DBH* than tropical secondary forests in Sarawak, Malaysia (Brown, 1997; Kenzo et al., 2009; Yen and Cochard, 2017). In contrast, cashew plantations show a significantly lower mean *DBH* compared to older counterparts in Kampong Cham, Cambodia (Avtar et al., 2013).

Aboveground and deadwood biomass

Our results support that land-cover conversion reduces in aboveground and deadwood biomass in regrowth forests and cashew plantations compared to evergreen forests. The substantial decline in aboveground biomass following conversion from EF to RF or CP is primarily driven by historical human disturbance, particularly clear-cutting and the removal of large trees, as evidenced by reduced *DBH* and tree height in this study. Similarly, *DWB* decreased as EF were replaced by RF and CP, reflecting the impacts of land-cover change on forest biodiversity and ecosystem health. *DWB* is a key indicator of biodiversity and ecosystem health, supporting various species and ecosystem processes like carbon and nitrogen cycling, soil fertility enhancement, pollination, and erosion control (Parisi et al., 2018a; Santopuoli et al., 2021; Tláskal et al., 2021). Variations in total *DWB* values could result from the degree of disturbances within the studied forests (Baker et al., 2007). The higher *DWB* in EF is due to its old stand age, long-term accumulation of *DWB*, and absence of slash-and-burn practice as observed in RF and CP (van Galen et al., 2019). In CP, some farmers periodically cut and burn dead branches of cashew trees to promote growth. Consistent with these trends, *DWB* in our EF and RF was comparable to previous studies in Cambodia and Malaysia (Saner et al., 2012; Kiyono et al., 2018), whereas our CP has less *DWB* than plantations in Cameroon (Victor et al., 2021).

Stem density and basal area

The land-cover change alters stem density across EF, RF, and CP. Our mean stem density per hectare of evergreen forests is consistent with previous studies in Cambodia, Vietnam, and in Borneo, while regrowth forests show lower densities compared to those in the Yucatan Peninsula, Mexico (Slik et al., 2010; Con et al., 2013; Román-Dañobeytia et al., 2014; Chheng et al., 2016; Theilade et al., 2022). Additionally, our stem density in cashew plantations is similar to that of Isuochi, Nigeria, but significantly greater than that of Casamance, Senegal, due to their differences in planting distance and management practices (Nzegbule et al., 2013; Ndiaye et al., 2020). The variation in stem density between evergreen forests and regrowth forests reflects distinctive stages of succession. In the early succession stage following clearance, open niches and resource abundance create a favourable environment for fast-growing and highly reproductive early-succession species, resulting in higher stem density and heightened interspecies competition (Zhang et al., 2020). As the forest matures, stem density naturally decreases as larger trees occupy more space, and take more of the light, water, and nutrient resources. This competition ultimately leads to the mortality of smaller trees, aligning with the power-law relationship between stem density and biomass commonly observed in mature forests (Mrad et al., 2020). This natural process also alters species composition, stand structure, habitat heterogeneity, and biomass of forests (Forrester et al., 2021). In cashew plantations, stem density is controlled by humans to enhance cashew yield. This alteration in stand structure complexity influences interspecies competition. These modifications also affect stand structure and interspecies competition, ultimately influencing the biodiversity and functioning of the ecosystem.

Also basal area decreases significantly when EF is replaced with RF or CP, impacting biomass, productivity, stand structure, and structural complexity (Gea-Izquierdo and Sánchez-González, 2022). RF has lower *BA* than EF, indicating early succession and disturbance (Ziegler, 2000). Despite tropical forests possess natural regenerative capabilities, RF may require several decades to achieve *BA* levels comparable to EF, highlighting the critical importance of conserving EF to maintain their ecological integrity and ecosystem services. In addition, the basal area of evergreen forests in our study aligns with those in northeast Cambodia and Pahang National Park, Malaysia, but falls below values reported for Laos, Cambodia's central plains and Vietnam's lowlands (Rundel, 1999; Sovu et al., 2009; Mohd Nazip, 2012; Chheng et al., 2016; Theilade et al., 2022). Our regrowth forest's *BA* exceeds that of regrowth forest in Laos, while cashew plantations surpass plantations in Tanzania's (Sovu et al., 2009; Malimbwi et al., 2016).

LAI* and *fPAR

LAI and *fPAR* differed markedly among the three land-cover classes, reflecting structural changes in canopy structure associated with land-cover conversion and consistent with our hypothesis. In our study, canopy leaf area index in evergreen forests surpasses that of dry evergreen forests in Kampong Thom, Cambodia, while regrowth forests lie between those of 18–35-year tropical secondary forests in Costa Rica; however, cashew plantations exceed reported values in India (Ito et al., 2007; Clark et al., 2021; Kumaresh et al., 2023). The LAI_C difference between the forests (EF and RF) and CP was significant due to CP management practices, resulting in a thin canopy with low LAI_C. In contrast, natural forests with their densely developed canopy have a high LAI_C. Additionally, LAI_C phenology followed the rainy and dry seasons, with peak values during the rainy season and low values during the dry season (Ito et al., 2007). During the dry season, reduced rainfall leads to less water availability for plant growth, causing plants to adapt to water stress by shedding their leaves, resulting in low LAI_C in the ecosystem (Maréchaux et al., 2018). The comparison between LAI_C and LAI_T of EF and RF with previous studies is presented in Table S9.3.

Our mean fraction of photosynthetically active radiation for EF and RF marginally exceeded the global range for broadleaf forests and the monthly range observed in the Amazon tropical forest in Santarém, Brazil (Senna et al., 2005; Pastorello et al., 2020). The *fPAR* for CP, on the other hand, is within the range values reported for broadleaf crops (Xiao et al., 2015). Despite annual variations in LAI_C (24 % for EF, 32 % for RF, 29 % for CP) and incoming solar irradiance, *fPAR* remained remarkably stable throughout the year in the forest ecosystems (EF and RF, Fig. 5). This stability can be attributed to the exponential relationship between *fPAR* and *LAI*, which typically saturates at *LAI* above 3 (Dawson et al., 2003). Our recorded lowest *LAI* for EF and RF was 3.48, likely contributing to this saturation and explaining the lack of phenology displayed in *fPAR*. The exclusion of reflected *PAR* above the canopy in the *fPAR* estimation may also contribute to the stability; however, previous studies have shown that the difference between intercepted (what we measured) and absorbed *PAR* (including the reflected component) is minimal (Olofsson and Eklundh, 2007).

Despite an increased stem density in RF compared to EF, similar canopy LAI and fPAR, our observations of significant differences in mean DBH, tree height and basal area, the reduction in aboveground and deadwood biomass, altered stem density, and reduction in contribution of understory LAI to total LAI, supports our hypothesis that the land-cover change causes a decreased complexity in stand structure.

4.5 Estimated Aboveground biomass based on *DBH-H* relationship

DBH-H relationship

Variation in the strength of *DBH-H* relationships reflects different disturbance histories in EF and RF, and the influence of management practices in CP. The *DBH-H* relationship is crucial for understanding variations in tree growth rates, successional stage, aboveground biomass, and forest health (Kramer et al., 2023). Finding a strong positive *DBH-H* relationship may indicate disturbances within the ecosystem, as these by initiating gaps in the canopy provide opportunities for fast-growing species to establish and utilize increased light availability and resources within the ecosystem (Senf et al., 2020). Hence, the observed relationships between EF and RF suggest a composition of fast-growing species and indicate that EF may have experienced past disturbances. Indeed, a windthrow in EF1 is reflected in its lowest LAI_C among EF plots and a smaller mean *DBH* (Table 1, Fig. S7.1a).

The lower *DBH-H* relationship in cashew plantations results from the growth strategy of the single species and management practices. In monocultures with uniformly aged cashew plants, competition for light and resources is comparable, resulting in a consistent resource distribution. Cashew's natural growth characteristics, with the species reaching up to 15 m in height and a *DBH* of 100 cm under favourable conditions (Avtar et al., 2014), indicate a preference for investing resources in branches and stems over height, especially in low-light competition environments. However, our observations indicate significant variation in the *DBH-H* relationship among CP plots (low R^2 value in Fig. 6, Fig. S7.2g–i) which may have been influenced by their different management practices, such as spacing, pruning, and thinning. These practices impact the *DBH-H* relationship by minimizing light competition, resulting in a higher *DBH-H* ratio which also affects the relationship (Deng et al., 2019; Bhandari et al., 2021).

Comparison of *AGB* estimation methods

Our results suggest that locally calibrated *DBH-H* relationships and wood density substantially affect *AGB* estimates compared to generalized models, supporting the feasibility of site-specific calibration, particularly for natural forest ecosystems. Recent studies have emphasized the significant uncertainty in estimating plot-level aboveground biomass when directly applying a generic *AGB* allometric equation (AGB_f) due to variations in species composition and stand structure between the study site and the equation's origin (Feldpausch et al., 2011; Burt et al., 2020). To address this challenge, our study proposes an allometric approach (AGB_h) using local species-specific wood density and the *DBH-H* relationship at the study site. This approach captures the unique characteristics of the site's species composition and stand structure (Ketterings et al., 2001a; Nyirambangutse et al., 2017). Our locally adopted AGB_h method produced estimates ~ 30 % higher than the generic AGB_f for both EF and RF (Table 3, Fig. 7b). This is likely due to the combined effects of higher mean wood density and a stronger *DBH* relationship, resulting in a more pronounced exponential growth response in *AGB* (Fig. 7a). Still, these ~ 30 % higher values align with the range reported in previous studies (Tables A2–A3). In contrast, in the CP case, our AGB_h method produced estimates less than a quarter of the generic AGB_f method. The reason is that the AGB_h method is less reliable when a weak *DBH-H* relationship is detected because it fails to accurately capture the overall tree size and volume. This is also reflected in the substantially larger uncertainty as indicated by the standardized errors of the parameters within the *DBH-H* relationship (Table A4, Table S7.4). The substantial difference between AGB_{wd} and AGB_f is primarily due to the wood density values used: 0.45 g cm^{-3} from Zanne et al. (2009) in this study versus 0.18 g cm^{-3} in the original AGB_f equation (Mlagalila, 2016), likely reflecting variation in cashew wood properties or wood density measurement protocols among the two studies. Despite clear differences in Fig. 7b, formal statistical comparisons were not conducted due to the limited number of plots per class (n = 3), which restricts statistical power. However, to fully validate the *AGB* allometric equations, destructive field-observed data would be necessary. Therefore, future research should include direct field measurements of *AGB* to more accurately validate the methods for these land-cover classes.

4.6 AGB_h relationships with LAI_T, SLA_{cwm} and S_R

Exploring the relationship between aboveground biomass and key ecosystem characteristics such as leaf area index, specific leaf area, and species richness is vital for comprehending the complexity of ecosystem dynamics and informing ecosystem modelling. We observed a strong positive relationship between LAI_T and AGB_h, supporting prior findings (He et al., 2021; Zhao et al., 2021). Higher LAI_T enhances light interception and results in higher biomass. Elevated AGB_h levels stimulate LAI_T expansion by providing resources for robust leaf growth, leading to a denser canopy and greater leaf coverage. Similarly, our findings support a positive relationship between SLA_{cwm} and AGB_h (Finegan et al., 2015; Ali et al., 2017; Gao et al., 2021). Higher SLA_{cwm} values indicate a plant community with improved photosynthetic capacity, nutrient uptake, and leaf turnover, which is essential for nutrient cycling (Reich et al., 1991). An increase in AGB_h has a reinforced effect on SLA_{cwm} values, suggesting enrichment of the soil nutrient pool and providing structural support for plant growth. This influences light availability and competition dynamics, affecting leaf morphology and SLA_{cwm}. Furthermore, the positive relationship between AGB_h and S_R is widely observed and explained by the niche complementarity hypothesis (Waide et al., 1999; Jactel et al., 2018; Steur et al., 2022). This concept suggests that an ecosystem with high species diversity has a greater variation in functional traits and resource-use strategies, lowering competition for scarce resources, and thus promoting productivity

(Tilman et al., 1997). In return, an increase in AGB_{h} fosters the coexistence of diverse species by providing more available resources and habitat complexity in an ecosystem, thereby increasing species richness.

5 Conclusions

In response to growing concerns over the ecological impacts of forest conversion in tropical Southeast Asia, we investigated how land-cover change from pristine evergreen forests to regrowth forests and cashew plantations alters stand structure, species diversity, functional traits, and soil conditions, and evaluated the feasibility of locally calibrated *DBH-H* allometries for improving aboveground biomass estimation. Our findings confirm our hypotheses that land-cover change reduces stand structural complexity, species composition, and leaf functional traits, and causes a substantial change in soil conditions. We further demonstrate the utility of our novel dataset for improving aboveground biomass estimation through the application of an allometric function based on locally specific wood density and the *DBH-H* relationship. This approach has great potential for improving carbon stock estimations and promoting informed forest management practices. However, as we lack direct destructive samples of aboveground biomass, we can neither reject nor support our second hypothesis that locally calibrated *DBH-H* relationships would substantially improve aboveground biomass estimates compared to generalized models. Moreover, our analysis of relationships between leaf area index, specific leaf area, species richness, and aboveground biomass, underlines land-cover change's profound impact on ecosystem productivity and functioning in these tropical forest regions. To strengthen and extend these findings, future studies should incorporate destructive sampling to validate our locally calibrated aboveground biomass allometric equations based on *DBH-H* relationships and wood density. Expanding field data collection by increasing the number and spatial distribution of plots across a broader range of land-use classes in tropical Southeast Asia and promoting open data sharing will be critical for improving our understanding of ecosystem responses to forest conversion and supporting sustainable forest management under global change in the region.

Appendix A

Table A1. Estimated lying deadwood biomass (Mg ha^{-1}), standing deadwood biomass (Mg ha^{-1}), and total deadwood biomass (Mg ha^{-1}) by different land-cover classes in Kulen. Mean ± SD is a mean plus or minus a standard deviation.

Land cover	Lying deadwood biomass (Mg ha^{-1})		Standing deadwood biomass (Mg ha^{-1})		Total deadwood biomass (Mg ha^{-1})	
	Mean ± SD	Range	Mean ± SD	Range	Mean ± SD	Range
EF (n = 3)	17.74 ± 19.93	1.64–40.03	9.74 ± 8.49	0–15.56	27.48 ± 12.37	15.31–40.03
RF (n = 3)	3.65 ± 5.32	0.48–9.79	1.16 ± 1.66	0–3.06	4.81 ± 6.97	0.48–12.85
CP (n = 3)	0.40 ± 0.19	0.28–0.62	0	0	0.40 ± 0.19	0.28–0.62

Table A2. Comparing estimated aboveground biomass (*AGB*, Mg ha^{-1}) in evergreen forests (EF) using adopted allometric equations (AGB_f), diameter at breast height (*DBH*) and tree height (*H*) power-law relationship (AGB_h), and previous *AGB* reported in previous studies. Mean ± SD is a mean plus or minus a standard deviation.

No.	Region	Vegetation type	*AGB* (Mg ha^{-1})		References
			Mean ± SD	Range	
1	Kulen, Cambodia	Tropical evergreen forest	311.66 ± 183.88	147.53–510.57	AGB_h in this study
2	Kulen, Cambodia	Tropical evergreen forest	238.53 ± 92.41	161.83–341.13	AGB_f in this study
3	Global	Tropical forest	379.02 ± 187.40	230.58–589.58	Chave et al. (2014)
4	Gia Lai, Vietnam	Tropical evergreen forest	273.24 ± 112.22	189.53–400.76	Nam et al. (2016)
5	Mondulkiri, Cambodia	Tropical moist evergreen forest	333.00 ± 137.00	78.00–837.00	Sola et al., (2014)
6	Borneo (Brunei, Malaysia, Indonesia)	Tropical lowland evergreen forest	458.16 ± 123.62	196.30–778.50	Slik et al. (2010))
7	Thanh Hoa, Vietnam	Tropical evergreen broadleaf forest	251.81 ± 125.43	40.88–543.88	Nguyen and Kappas (2020)
8	Africa	Tropical evergreen forest	429.00	114.00–749.00	Lewis et al. (2013)
9	Cambodia	Evergreen forest	243.00 ± 128.00	11.00–837.00	Sola et al., (2014)
10	Kampong Thom, Cambodia	Evergreen forest	294.00 ± 65.00	176.00–398.00	Ota et al. (2015)
11	Vietnam	Tropical evergreen broadleaf forests in various ecoregions	230.10 ± 8.60	199.00–320.20	Van Do et al. (2019)

Table A3. Comparing estimated aboveground biomass (*AGB*, Mg ha^{-1}) in regrowth forests (RF) using adopted allometric equations (AGB_f), diameter at breast height (*DBH*) and tree height (*H*) power-law relationship (AGB_h), and previous *AGB* reported in previous studies. Mean ± SD is a mean plus or minus a standard deviation.

No.	Region	Vegetation type	*AGB* (Mg ha^{-1})		References
			Mean ± SD	Range	
1	Kulen, Cambodia	Natural regrowth evergreen forest	54.19 ± 14.09	38.26–65.04	AGB_h in this study
2	Kulen, Cambodia	Natural regrowth evergreen forest	41.66 ± 9.82	31.60–51.21	AGB_f in this study
3	Sumatra, Indonesia	Mixed secondary forest	59.04 ± 17.15	39.26–69.79	Ketterings et al. (2001a)
4	Kampong Thom, Cambodia	Regrowth forest	42.00 ± 21.00	22.00–90.00	Ota et al. (2015)
5	Malaysia	Young forests aged 8.5–17 years	63.60 ± 34.93	34.00–118.00	Kho and Jepsen (2015)

Table A4. Comparing estimated aboveground biomass (*AGB*, Mg ha^{-1}) in cashew plantations (CP) using adopted allometric equations (AGB_f), diameter at breast height (*DBH*) and tree height (*H*) power-law relationship (AGB_h), and previous *AGB* reported in previous studies. Mean ± SD is a mean plus or minus a standard deviation.

No.	Region	Vegetation type	*AGB* (Mg ha^{-1})		References
			Mean ± SD	Range	
1	Kulen, Cambodia	Family-scale cashew plantation	16.70 ± 4.80	11.23–20.23	AGB_h in this study
2	Kulen, Cambodia	Family-scale cashew plantation	70.60 ± 22.01	46.16–88.87	AGB_f in this study
3	Benin	Cashew agroforestry farming	18.07 ± 2.14	-	Biah et al. (2019)
4	Guinean, Cote d'Ivoire	Cashew plantation	13.78 ± 0.98	-	Kanmegne Tamga et al. (2022)
5	Kampong Cham, Cambodia	Large-scale and intensively managed cashew plantation (10–16 years of age)	104.30 ± 19.65	72.00–143.00	Avtar et al. (2013)

Data availability

All the collected data used in this study are publicly available via the links as follows:

1. The datasets of the forest inventory, leaf area index, and leaf functional traits across various land-cover classes are available at https://doi.org/10.5281/zenodo.10146582 (Sovann et al., 2024a).
2. The daily data, including *fPAR*, soil conditions, and meteorological conditions from April 10, 2022, to April 9, 2023, can be downloaded from https://doi.org/10.5281/zenodo.10159726 (Sovann et al., 2024b).
3. Future data from the field site will be uploaded to https://zenodo.org/communities/cambodia_ecosystem_data on a regular basis.

Author contribution

CS led field data collection, analysis, and manuscript writing. TT and SO contributed to conceptualization, manuscript review, editing, and supervision. SK and SS provided administrative support and supervised fieldwork in Cambodia. PV offered technical guidance and support in equipment installation and maintenance. SB managed field data collection. All authors contributed to editing the manuscript.

Competing interests

The authors declare no conflict of interest.

Acknowledgements

This work was supported by the Swedish International Development Cooperation Agency through the "Sweden-Royal University of Phnom Penh Bilateral program" (Contribution Number: 11599). Tagesson was additionally funded by the Swedish National Space Agency (SNSA Dnr: 2021-00144) and Formas (Dnr. 2021-00644; 2023-02436). The research presented in this paper is a contribution to the Strategic Research Area "Biodiversity and Ecosystem Services in a Changing Climate", BECC, funded by the Swedish government.

We are grateful to the Ministry of Environment (Cambodia) and Siem Reap Provincial Administration for their grant permissions, administrative support, and accommodation during our fieldwork. A special note of thanks goes to Seng Saingheat for his dedication and leadership, along with his ranger colleagues, including Sou Sy, Let Chey, Khun Chi, Soun Sao, Kroem Veng, Choun Choy, and Ti Has. Sincere appreciation to the research teams from the Royal University of Agriculture (Cambodia), namely Horn Sarun, Yorn Chomroeun, Sok Pheak, Sum Dara, and Long Sotheara, for their invaluable support in forest inventory. We greatly appreciate Mot Ly and Chim Lychheng, as well as Rum Pheara, Svay Chanboth, and Mach Sokmean, for their support throughout our data collection journey.

References

Akossou, A. Y. J., Salifou, A. D., Tchiwanou, L. A., Assani Saliou, S. A., and Azoua, M. H.: Area and Dry Mass Estimation of Cashew (Anacardium Occidentale) Leaves: Effect of Tree Position within a Plantation around Parakou, Benin, Journal of Experimental Agriculture International, 15, 1-12, https://doi.org/10.9734/JEAI/2017/29798, 2016.

Akram, M. A., Wang, X., Shrestha, N., Zhang, Y., Sun, Y., Yao, S., Li, J., Hou, Q., Hu, W., Ran, J., and Deng, J.: Variations and Driving Factors of Leaf Functional Traits in the Dominant Desert Plant Species Along an Environmental Gradient in the Drylands of China, Sci Total Environ, 897, 165394, https://doi.org/10.1016/j.scitotenv.2023.165394, 2023.

Ali, A., Yan, E. R., Chang, S. X., Cheng, J. Y., and Liu, X. Y.: Community-Weighted Mean of Leaf Traits and Divergence of Wood Traits Predict Aboveground Biomass in Secondary Subtropical Forests, Sci Total Environ, 574, 654-662, https://doi.org/10.1016/j.scitotenv.2016.09.022, 2017.

Austin, A. T., Yahdjian, L., Stark, J. M., Belnap, J., Porporato, A., Norton, U., Ravetta, D. A., and Schaeffer, S. M.: Water Pulses and Biogeochemical Cycles in Arid and Semiarid Ecosystems, Oecologia, 141, 221-235, https://doi.org/10.1007/s00442-004-1519-1, 2004.

Avtar, R., Suzuki, R., and Sawada, H.: Natural Forest Biomass Estimation Based on Plantation Information Using Palsar Data, PLoS One, 9, e86121, https://doi.org/10.1371/journal.pone.0086121, 2014.

Avtar, R., Takeuchi, W., and Sawada, H.: Monitoring of Biophysical Parameters of Cashew Plants in Cambodia Using Alos/Palsar Data, Environ Monit Assess, 185, 2023-2037, https://doi.org/10.1007/s10661-012-2685-y, 2013.

Baker, T. R., Honorio Coronado, E. N., Phillips, O. L., Martin, J., van der Heijden, G. M. F., Garcia, M., and Silva Espejo, J.: Low Stocks of Coarse Woody Debris in a Southwest Amazonian Forest, Oecologia, 152, 495-504, https://doi.org/10.1007/s00442-007-0667-5, 2007.

Barlow, J., Lennox, G. D., Ferreira, J., Berenguer, E., Lees, A. C., Mac Nally, R., Thomson, J. R., Ferraz, S. F., Louzada, J., Oliveira, V. H., Parry, L., Solar, R. R., Vieira, I. C., Aragao, L. E., Begotti, R. A., Braga, R. F., Cardoso, T. M., de Oliveira, R. C., Jr., Souza, C. M., Jr., Moura, N. G., Nunes, S. S., Siqueira, J. V., Pardini, R., Silveira, J. M., Vaz-de-Mello, F. Z., Veiga, R. C., Venturieri, A., and Gardner, T. A.: Anthropogenic Disturbance in Tropical Forests Can Double Biodiversity Loss from Deforestation, Nature, 535, 144-147, https://doi.org/10.1038/nature18326, 2016.

Bezerra, M. A., Lacerda, C. F. D., Gomes Filho, E., Abreu, C. E. B. D., and Prisco, J. T.: Physiology of Cashew Plants Grown under Adverse Conditions, Brazilian Journal of Plant Physiology, 19, 449-461, https://doi.org/10.1590/s1677-04202007000400012, 2007.

Bhandari, S. K., Veneklaas, E. J., McCaw, L., Mazanec, R., Whitford, K., and Renton, M.: Effect of Thinning and Fertilizer on Growth and Allometry Of, Forest Ecology and Management, 479, 118594, https://doi.org/10.1016/j.foreco.2020.118594, 2021.

Biah, I., Guendehou, S., Goussanou, C., Kaire, M., and Sinsin, B.: Allometric Models for Estimating Biomass Stocks in Cashew (Linnaeus) Plantation in Benin, 2019.

Brown, S.: Estimating Biomass and Biomass Change of Tropical Forests: A Primer, Food and Agriculture Organization of the United Nations, 1997.

Burt, A., Calders, K., Cuni-Sanchez, A., Gómez-Dans, J., Lewis, P., Lewis, S. L., Malhi, Y., Phillips, O. L., and Disney, M.: Assessment of Bias in Pan-Tropical Biomass Predictions, 3, https://doi.org/10.3389/ffgc.2020.00012, 2020.

Cardinale, B. J., Duffy, J. E., Gonzalez, A., Hooper, D. U., Perrings, C., Venail, P., Narwani, A., Mace, G. M., Tilman, D., Wardle, D. A., Kinzig, A. P., Daily, G. C., Loreau, M., Grace, J. B., Larigauderie, A., Srivastava, D. S., and Naeem, S.: Biodiversity Loss and Its Impact on Humanity, Nature, 486, 59-67, https://doi.org/10.1038/nature11148, 2012.

Chave, J., Andalo, C., Brown, S., Cairns, M. A., Chambers, J. Q., Eamus, D., Folster, H., Fromard, F., Higuchi, N., Kira, T., Lescure, J. P., Nelson, B. W., Ogawa, H., Puig, H., Riera, B., and Yamakura, T.: Tree Allometry and Improved Estimation of Carbon Stocks and Balance in Tropical Forests, Oecologia, 145, 87-99, https://doi.org/10.1007/s00442-005-0100-x, 2005.

Chave, J., Rejou-Mechain, M., Burquez, A., Chidumayo, E., Colgan, M. S., Delitti, W. B., Duque, A., Eid, T., Fearnside, P. M., Goodman, R. C., Henry, M., Martinez-Yrizar, A., Mugasha, W. A., Muller-Landau, H. C., Mencuccini, M., Nelson, B. W., Ngomanda, A., Nogueira, E. M., Ortiz-Malavassi, E., Pelissier, R., Ploton, P., Ryan, C. M., Saldarriaga, J. G., and Vieilledent, G.: Improved Allometric Models to Estimate the Aboveground Biomass of Tropical Trees, Glob Chang Biol, 20, 3177-3190, https://doi.org/10.1111/gcb.12629, 2014.

Chen, B. Q., Li, X. P., Xiao, X. M., Zhao, B., Dong, J. W., Kou, W. L., Qin, Y. W., Yang, C., Wu, Z. X., Sun, R., Lan, G. Y., and Xie, G. S.: Mapping Tropical Forests and Deciduous Rubber Plantations in Hainan Island, China by Integrating Palsar 25-M and Multi-Temporal Landsat Images, International Journal of Applied Earth Observation and Geoinformation, 50, 117-130, https://doi.org/10.1016/j.jag.2016.03.011, 2016.

Chheng, K., Sasaki, N., Mizoue, N., Khorn, S., Kao, D., and Lowe, A.: Assessment of Carbon Stocks of Semi-Evergreen Forests in Cambodia, Global Ecology and Conservation, 5, 34-47, https://doi.org/10.1016/j.gecco.2015.11.007, 2016.

Chim, K., Tunnicliffe, J., Shamseldin, A., and Ota, T.: Land Use Change Detection and Prediction in Upper Siem Reap River, Cambodia, Hydrology, 6, 64, https://doi.org/10.3390/hydrology6030064, 2019.

Chim, K., Tunnicliffe, J., Shamseldin, A., and Sarun, S.: Sustainable Water Management in the Angkor Temple Complex, Cambodia, Sn Applied Sciences, 3, https://doi.org/10.1007/s42452-020-04030-0, 2021.

Clark, D. B., Oberbauer, S. F., Clark, D. A., Ryan, M. G., and Dubayah, R. O.: Physical Structure and Biological Composition of Canopies in Tropical Secondary and Old-Growth Forests, PLoS One, 16, e0256571, https://doi.org/10.1371/journal.pone.0256571, 2021.

Con, T. V., Thang, N. T., Ha, D. T. T., Khiem, C. C., Quy, T. H., Lam, V. T., Van Do, T., and Sato, T.: Relationship between Aboveground Biomass and Measures of Structure and Species Diversity in Tropical Forests of Vietnam, Forest Ecology and Management, 310, 213-218, https://doi.org/10.1016/j.foreco.2013.08.034, 2013.

Coste, S., Baraloto, C., Leroy, C., Marcon, É., Renaud, A., Richardson, A. D., Roggy, J. C., Schimann, H., Uddling, J., and Hérault, B.: Assessing Foliar Chlorophyll Contents with the Spad-502 Chlorophyll Meter: A Calibration Test with Thirteen Tree Species of Tropical Rainforest in French Guiana, Annals of Forest Science, 67, 607-607, https://doi.org/10.1051/forest/2010020, 2010.

Dawson, T. P., North, P. R. J., Plummer, S. E., and Curran, P. J.: Forest Ecosystem Chlorophyll Content: Implications for Remotely Sensed Estimates of Net Primary Productivity, International Journal of Remote Sensing, 24, 611-617, https://doi.org/10.1080/01431160304984, 2003.

Deng, C., Zhang, S. G., Lu, Y. C., Froese, R. E., Ming, A. G., and Li, Q. F.: Thinning Effects on the Tree Height–Diameter Allometry of Masson Pine (Pinus Massoniana Lamb.), Forests, 10, 1129, https://doi.org/10.3390/f10121129, 2019.

Díaz, S., Lavorel, S., De Bello, F., Quétier, F., Grigulis, K., and Robson, T. M.: Incorporating Plant Functional Diversity Effects in Ecosystem Service Assessments, Proceedings of the National Academy of Sciences, 104, 20684-20689, https://doi.org/10.1073/pnas.0704716104, 2007.

Fan, F., Li, W., Feng, Z., and Yang, Y.: Combining Landscape Patterns and Ecosystem Services to Disclose Ecosystem Changes in Tropical Cropland-Forest Shifting Zones: Inspiration from Mainland Southeast Asia, Journal of Cleaner Production, 434, 140058, https://doi.org/https://doi.org/10.1016/j.jclepro.2023.140058, 2024.

Fang, H., Baret, F., Plummer, S., and Schaepman-Strub, G.: An Overview of Global Leaf Area Index (Lai): Methods, Products, Validation, and Applications, Reviews of Geophysics, 57, 739-799, https://doi.org/https://doi.org/10.1029/2018RG000608, 2019.

Feldpausch, T. R., Banin, L., Phillips, O. L., Baker, T. R., Lewis, S. L., Quesada, C. A., Affum-Baffoe, K., Arets, E. J. M. M., Berry, N. J., Bird, M., Brondizio, E. S., de Camargo, P., Chave, J., Djagbletey, G., Domingues, T. F., Drescher, M., Fearnside, P. M., França, M. B., Fyllas, N. M., Lopez-Gonzalez, G., Hladik, A., Higuchi, N., Hunter, M. O., Iida, Y., Salim, K. A., Kassim, A. R., Keller, M., Kemp, J., King, D. A., Lovett, J. C., Marimon, B. S., Marimon, B. H., Lenza, E., Marshall, A. R., Metcalfe, D. J., Mitchard, E. T. A., Moran, E. F., Nelson, B. W., Nilus, R., Nogueira, E. M., Palace, M., Patiño, S., Peh, K. S. H., Raventos, M. T., Reitsma, J. M., Saiz, G., Schrodt, F., Sonké, B., Taedoumg, H. E., Tan, S., White, L., Wöll, H., and Lloyd, J.: Height-Diameter Allometry of Tropical Forest Trees, Biogeosciences, 8, 1081-1106, https://doi.org/10.5194/bg-8-1081-2011, 2011.

Feng, X., Uriarte, M., Gonzalez, G., Reed, S., Thompson, J., Zimmerman, J. K., and Murphy, L.: Improving Predictions of Tropical Forest Response to Climate Change through Integration of Field Studies and Ecosystem Modeling, Glob Chang Biol, 24, e213-e232, https://doi.org/10.1111/gcb.13863, 2018.

Fichtner, A. and Härdtle, W.: Forest Ecosystems: A Functional and Biodiversity Perspective, in: Perspectives for Biodiversity and Ecosystems, Environmental Challenges and Solutions, Springer International Publishing, 383-405, https://doi.org/10.1007/978-3-030-57710-0_16, 2021.

Finegan, B., Peña-Claros, M., de Oliveira, A., Ascarrunz, N., Bret-Harte, M. S., Carreño-Rocabado, G., Casanoves, F., Díaz, S., Eguiguren Velepucha, P., Fernandez, F., Licona, J. C., Lorenzo, L., Salgado Negret, B., Vaz, M., and Poorter, L.: Does Functional Trait Diversity Predict above-Ground Biomass and Productivity of Tropical Forests? Testing Three Alternative Hypotheses, 103, 191-201, https://doi.org/10.1111/1365-2745.12346, 2015.

Forrester, D. I., Baker, T. G., Elms, S. R., Hobi, M. L., Ouyang, S., Wiedemann, J. C., Xiang, W., Zell, J., and Pulkkinen, M.: Self-Thinning Tree Mortality Models That Account for Vertical Stand Structure, Species Mixing and Climate, Forest Ecology and Management, 487, 118936, https://doi.org/10.1016/j.foreco.2021.118936, 2021.

Galanes, I. T. and Thomlinson, J. R.: Relationships between Spatial Configuration of Tropical Forest Patches and Woody Plant Diversity in Northeastern Puerto Rico, Plant Ecol, 201, 101-113, https://doi.org/10.1007/s11258-008-9475-1, 2009.

Gamon, J. A., Coburn, C., Flanagan, L. B., Huemmrich, K. F., Kiddle, C., Sanchez-Azofeifa, G. A., Thayer, D. R., Vescovo, L., Gianelle, D., Sims, D. A., Rahman, A. F., and Pastorello, G. Z.: Specnet Revisited: Bridging Flux and Remote Sensing Communities, Canadian Journal of Remote Sensing, 36, S376-S390, https://doi.org/10.5589/m10-067, 2010.

Gao, J., Wang, K., and Zhang, X.: Patterns and Drivers of Community Specific Leaf Area in China, Global Ecology and Conservation, 33, e01971, https://doi.org/10.1016/j.gecco.2021.e01971, 2022.

Gao, W.-Q., Lei, X.-D., Gao, D.-L., and Li, Y.-T.: Mass-Ratio and Complementarity Effects Simultaneously Drive Aboveground Biomass in Temperate Quercus Forests through Stand Structure, 11, 16806-16816, https://doi.org/10.1002/ece3.8312, 2021.

Gardner, T. A., Barlow, J., Chazdon, R., Ewers, R. M., Harvey, C. A., Peres, C. A., and Sodhi, N. S.: Prospects for Tropical Forest Biodiversity in a Human-Modified World, Ecol Lett, 12, 561-582, https://doi.org/10.1111/j.1461-0248.2009.01294.x, 2009.

Garnier, E., Shipley, B., Roumet, C., and Laurent, G.: A Standardized Protocol for the Determination of Specific Leaf Area and Leaf Dry Matter Content, Functional Ecology, 15, 688-695, https://doi.org/10.1046/j.0269-8463.2001.00563.x, 2001.

Garnier, E., Cortez, J., Billès, G., Navas, M. L., Roumet, C., Debussche, M., Laurent, G., Blanchard, A., Aubry, D., Bellmann, A., Neill, C., and Toussaint, J. P.: Plant Functional Markers Capture Ecosystem Properties during Secondary Succession, Ecology, 85, 2630-2637, https://doi.org/10.1890/03-0799, 2004.

Gea-Izquierdo, G. and Sánchez-González, M.: Forest Disturbances and Climate Constrain Carbon Allocation Dynamics in Trees, 28, 4342-4358, https://doi.org/10.1111/gcb.16172, 2022.

Geissler, P., Hartmann, T., Ihlow, F., Neang, T., Seng, R., Wagner, P., and Bohme, W.: Herpetofauna of the Phnom Kulen, Cambodian Journal of Natural History, 40, 2019.

Geng, J., Li, H., Pang, J., Zhang, W., and Shi, Y.: The Effects of Land-Use Conversion on Evapotranspiration and Water Balance of Subtropical Forest and Managed Tea Plantation in Taihu Lake Basin, China, 36, e14652, https://doi.org/10.1002/hyp.14652, 2022.

Giam, X.: Global Biodiversity Loss from Tropical Deforestation, Proc Natl Acad Sci U S A, 114, 5775-5777, https://doi.org/10.1073/pnas.1706264114, 2017.

Gloor, M., Brienen, R. J. W., Galbraith, D., Feldpausch, T. R., Schöngart, J., Guyot, J. L., Espinoza, J. C., Lloyd, J., and Phillips, O. L.: Intensification of the Amazon Hydrological Cycle over the Last Two Decades, Geophysical Research Letters, 40, 1729-1733, https://doi.org/10.1002/grl.50377, 2013.

Green, J. K., Berry, J., Ciais, P., Zhang, Y., and Gentine, P.: Amazon Rainforest Photosynthesis Increases in Response to Atmospheric Dryness, 6, eabb7232, https://doi.org/10.1126/sciadv.abb7232, 2020.

Grogan, K., Pflugmacher, D., Hostert, P., Kennedy, R., and Fensholt, R.: Cross-Border Forest Disturbance and the Role of Natural Rubber in Mainland Southeast Asia Using Annual Landsat Time Series, Remote Sensing of Environment, 169, 438-453, https://doi.org/10.1016/j.rse.2015.03.001, 2015.

Guerrieri, R., Correia, M., Martín-Forés, I., Alfaro-Sánchez, R., Pino, J., Hampe, A., Valladares, F., and Espelta, J. M.: Land-Use Legacies Influence Tree Water-Use Efficiency and Nitrogen Availability in Recently Established European Forests, Functional Ecology, 35, 1325-1340, https://doi.org/10.1111/1365-2435.13787, 2021.

Guo, H., Duan, D., Lei, H., Chen, Y., Li, J., Albasher, G., and Li, X.: Environmental Drivers of Landscape Fragmentation Influence Intraspecific Leaf Traits in Forest Ecosystem, Forests, 14, 1875, https://doi.org/10.3390/f14091875, 2023a.

Guo, J., Feng, H., McNie, P., Liu, Q., Xu, X., Pan, C., Yan, K., Feng, L., Adehanom Goitom, E., and Yu, Y.: Species Mixing Improves Soil Properties and Enzymatic Activities in Chinese Fir Plantations: A Meta-Analysis, CATENA, 220, 106723, https://doi.org/10.1016/j.catena.2022.106723, 2023b.

Ha, V.: Forest Fragmentation in Vietnam: Effects on Tree Diversity, Populations and Genetics, Utrecht University, 2015.

Hang, P., Ishwaran, N., Hong, T., and Delanghe, P.: From Conservation to Sustainable Development—a Case Study of Angkor World Heritage Site, Cambodia, Journal of Environmental Science and Engineering A, 5, 141-155, https://doi.org/10.17265/2162-5298/2016.03.004, 2016.

Hansen, M. C., Potapov, P. V., Moore, R., Hancher, M., Turubanova, S. A., Tyukavina, A., Thau, D., Stehman, S. V., Goetz, S. J., Loveland, T. R., Kommareddy, A., Egorov, A., Chini, L., Justice, C. O., and Townshend, J. R.: High-Resolution Global Maps of 21st-Century Forest Cover Change, Science, 342, 850-853, https://doi.org/10.1126/science.1244693, 2013.

He, L. M., Wang, R., Mostovoy, G., Liu, J. E., Chen, J. M., Shang, J. L., Liu, J. G., McNairn, H., and Powers, J.: Crop Biomass Mapping Based on Ecosystem Modeling at Regional Scale Using High Resolution Sentinel-2 Data, Remote Sensing, 13, 806, https://doi.org/10.3390/rs13040806, 2021.

Hector, A.: The Effect of Diversity on Productivity: Detecting the Role of Species Complementarity, Oikos, 82, 597-599, https://doi.org/10.2307/3546380, 1998.

Hill, M. O.: Diversity and Evenness: A Unifying Notation and Its Consequences, Ecology, 54, 427-432, https://doi.org/10.2307/1934352, 1973.

Horel, Á., Zsigmond, T., Molnár, S., Zagyva, I., and Bakacsi, Z.: Long-Term Soil Water Content Dynamics under Different Land Uses in a Small Agricultural Catchment, Journal of Hydrology and Hydromechanics, 70, 284-294, https://doi.org/10.2478/johh-2022-0015, 2022.

Howell, S. R., Song, G.-Z. M., Chao, K.-J., Doley, D., and Camac, J.: Functional Evaluation of Height–Diameter Relationships and Tree Development in an Australian Subtropical Rainforest, Australian Journal of Botany, 70, 158-173, https://doi.org/10.1071/bt21049, 2022.

Huxley, J.: Problems of Relative Growth, L. MacVeagh, The Dial Press, New York, 1932.

Ibrahim, H. M. and Alghamdi, A. G.: Effect of the Particle Size of Clinoptilolite Zeolite on Water Content and Soil Water Storage in a Loamy Sand Soil, 13, 607, 2021.

Icraf Database: http://db.worldagroforestry.org/, last access: 21 May 2022.

Ito, E., Khorn, S., Lim, S., Pol, S., Tith, B., Pith, P., Tani, A., Kanzaki, M., Kaneko, T., Okuda, Y., Kabeya, N., Nobuhiro, T., and Araki, M.: Comparison of the Leaf Area Index (Lai) of Two Types of Dipterocarp Forest on the West Bank of the Mekong River, Cambodia, Forest Environments in the Mekong River Basin, 214-+, https://doi.org/10.1007/978-4-431-46503-4_19, 2007.

Jacobson, C., Smith, J., Sou, S., Nielsen, C., and Hang, P.: Effective Water Management for Landscape Management in the Siem Reap Catchment, Cambodia, in: Biodiversity-Health-Sustainability Nexus in Socio-Ecological Production Landscapes and Seascapes (Sepls), Satoyama Initiative Thematic Review, Springer Nature Singapore, 129-150, https://doi.org/10.1007/978-981-16-9893-4_7, 2022.

Jactel, H., Gritti, E. S., Drossler, L., Forrester, D. I., Mason, W. L., Morin, X., Pretzsch, H., and Castagneyrol, B.: Positive Biodiversity-Productivity Relationships in Forests: Climate Matters, Biol Lett, 14, 20170747, https://doi.org/10.1098/rsbl.2017.0747, 2018.

Johansson, E., Olin, S., and Seaquist, J.: Foreign Demand for Agricultural Commodities Drives Virtual Carbon Exports from Cambodia, Environmental Research Letters, 15, 064034, https://doi.org/10.1088/1748-9326/ab8157, 2020.

Kanmegne Tamga, D., Latifi, H., Ullmann, T., Baumhauer, R., Bayala, J., and Thiel, M.: Estimation of Aboveground Biomass in Agroforestry Systems over Three Climatic Regions in West Africa Using Sentinel-1, Sentinel-2, Alos, and Gedi Data, Sensors (Basel), 23, 349, https://doi.org/10.3390/s23010349, 2022.

Kattge, J. and Bonisch, G. and Diaz, S. and Lavorel, S. and Prentice, I. C. and Leadley, P. and Tautenhahn, S. and Werner, G. D. A. and Aakala, T. and Abedi, M. and Acosta, A. T. R. and Adamidis, G. C. and Adamson, K. and Aiba, M. and Albert, C. H. and Alcantara, J. M. and Alcazar, C. C. and Aleixo, I. and Ali, H. and Amiaud, B. and Ammer, C. and Amoroso, M. M. and Anand, M. and Anderson, C. and Anten, N. and Antos, J. and Apgaua, D. M. G. and Ashman, T. L. and Asmara, D. H. and Asner, G. P. and Aspinwall, M. and Atkin, O. and Aubin, I. and Baastrup-Spohr, L. and Bahalkeh, K. and Bahn, M. and Baker, T. and Baker, W. J. and Bakker, J. P. and Baldocchi, D. and Baltzer, J. and Banerjee, A. and Baranger, A. and Barlow, J. and Barneche, D. R. and Baruch, Z. and Bastianelli, D. and Battles, J. and Bauerle, W. and Bauters, M. and Bazzato, E. and Beckmann, M. and Beeckman, H. and Beierkuhnlein, C. and Bekker, R. and Belfry, G. and Belluau, M. and Beloiu, M. and Benavides, R. and Benomar, L. and Berdugo-Lattke, M. L. and Berenguer, E. and Bergamin, R. and Bergmann, J. and Bergmann Carlucci, M. and Berner, L. and Bernhardt-Romermann, M. and Bigler, C. and Bjorkman, A. D. and Blackman, C. and Blanco, C. and Blonder, B. and Blumenthal, D. and Bocanegra-Gonzalez, K. T. and Boeckx, P. and Bohlman, S. and Bohning-Gaese, K. and Boisvert-Marsh, L. and Bond, W. and Bond-Lamberty, B. and Boom, A. and Boonman, C. C. F. and Bordin, K. and Boughton, E. H. and Boukili, V. and Bowman, D. and Bravo, S. and Brendel, M. R. and Broadley, M. R. and Brown, K. A. and Bruelheide, H. and Brumnich, F. and Bruun, H. H. and Bruy, D. and Buchanan, S. W. and Bucher, S. F. and Buchmann, N. and Buitenwerf, R. and Bunker, D. E. and Burger, J. and Burrascano, S. and Burslem, D. and Butterfield, B. J. and Byun, C. and Marques, M. and Scalon, M. C. and Caccianiga, M. and Cadotte, M. and Cailleret, M. and Camac, J. and Camarero, J. J. and Campany, C. and Campetella, G. and Campos, J. A. and Cano-Arboleda, L. and Canullo, R. and Carbognani, M. and Carvalho, F. and Casanoves, F. and Castagneyrol, B. and Catford, J. A. and Cavender-Bares, J. and Cerabolini, B. E. L. and Cervellini, M. and Chacon-Madrigal, E. and Chapin, K. and Chapin, F. S. and Chelli, S. and Chen, S. C. and Chen, A. and Cherubini, P. and Chianucci, F. and Choat, B. and Chung, K. S. and Chytry, M. and Ciccarelli, D. and Coll, L. and Collins, C. G. and Conti, L. and Coomes, D. and Cornelissen, J. H. C. and Cornwell, W. K. and Corona, P. and Coyea, M. and Craine, J. and Craven, D. and Cromsigt, J. and Csecserits, A. and Cufar, K. and Cuntz, M. and da Silva, A. C. and Dahlin, K. M. and Dainese, M. and Dalke, I. and Dalle Fratte, M. and Dang-Le, A. T. and Danihelka, J. and Dannoura, M. and Dawson, S. and de Beer, A. J. and De Frutos, A. and De Long, J. R. and Dechant, B. and Delagrange, S. and Delpierre, N. and Derroire, G. and Dias, A. S. and Diaz-Toribio, M. H. and Dimitrakopoulos, P. G. and Dobrowolski, M. and Doktor, D. and Drevojan, P. and Dong, N. and Dransfield, J. and Dressler, S. and Duarte, L. and Ducouret, E. and Dullinger, S. and Durka, W. and Duursma, R. and Dymova, O. and A, E. V. and Eckstein, R. L. and Ejtehadi, H. and Elser, J. and Emilio, T. and Engemann, K. and Erfanian, M. B.

and Erfmeier, A. and Esquivel-Muelbert, A. and Esser, G. and Estiarte, M. and Domingues, T. F. and Fagan, W. F. and Fagundez, J. and Falster, D. S. and Fan, Y. and Fang, J. and Farris, E. and Fazlioglu, F. and Feng, Y. and Fernandez-Mendez, F. and Ferrara, C. and Ferreira, J. and Fidelis, A. and Finegan, B. and Firn, J. and Flowers, T. J. and Flynn, D. F. B. and Fontana, V. and Forey, E. and Forgiarini, C. and Francois, L. and Frangipani, M. and Frank, D. and Frenette-Dussault, C. and Freschet, G. T. and Fry, E. L. and Fyllas, N. M. and Mazzochini, G. G. and Gachet, S. and Gallagher, R. and Ganade, G. and Ganga, F. and Garcia-Palacios, P. and Gargaglione, V. and Garnier, E. and Garrido, J. L. and de Gasper, A. L. and Gea-Izquierdo, G. and Gibson, D. and Gillison, A. N. and Giroldo, A. and Glasenhardt, M. C. and Gleason, S. and Gliesch, M. and Goldberg, E. and Goldel, B. and Gonzalez-Akre, E. and Gonzalez-Andujar, J. L. and Gonzalez-Melo, A. and Gonzalez-Robles, A. and Graae, B. J. and Granda, E. and Graves, S. and Green, W. A. and Gregor, T. and Gross, N. and Guerin, G. R. and Gunther, A. and Gutierrez, A. G. and Haddock, L. and Haines, A. and Hall, J. and Hambuckers, A. and Han, W. and Harrison, S. P. and Hattingh, W. and Hawes, J. E. and He, T. and He, P. and Heberling, J. M. and Helm, A. and Hempel, S. and Hentschel, J. and Herault, B. and Heres, A. M. and Herz, K. and Heuertz, M. and Hickler, T. and Hietz, P. and Higuchi, P. and Hipp, A. L. and Hirons, A. and Hock, M. and Hogan, J. A. and Holl, K. and Honnay, O. and Hornstein, D. and Hou, E. and Hough-Snee, N. and Hovstad, K. A. and Ichie, T. and Igic, B. and Illa, E. and Isaac, M. and Ishihara, M. and Ivanov, L. and Ivanova, L. and Iversen, C. M. and Izquierdo, J. and Jackson, R. B. and Jackson, B. and Jactel, H. and Jagodzinski, A. M. and Jandt, U. and Jansen, S. and Jenkins, T. and Jentsch, A. and Jespersen, J. R. P. and Jiang, G. F. and Johansen, J. L. and Johnson, D. and Jokela, E. J. and Joly, C. A. and Jordan, G. J. and Joseph, G. S. and Junaedi, D. and Junker, R. R. and Justes, E. and Kabzems, R. and Kane, J. and Kaplan, Z. and Kattenborn, T. and Kavelenova, L. and Kearsley, E. and Kempel, A. and Kenzo, T. and Kerkhoff, A. and Khalil, M. I. and Kinlock, N. L. and Kissling, W. D. and Kitajima, K. and Kitzberger, T. and Kjoller, R. and Klein, T. and Kleyer, M. and Klimesova, J. and Klipel, J. and Kloeppel, B. and Klotz, S. and Knops, J. M. H. and Kohyama, T. and Koike, F. and Kollmann, J. and Komac, B. and Komatsu, K. and Konig, C. and Kraft, N. J. B. and Kramer, K. and Kreft, H. and Kuhn, I. and Kumarathunge, D. and Kuppler, J. and Kurokawa, H. and Kurosawa, Y. and Kuyah, S. and Laclau, J. P. and Lafleur, B. and Lallai, E. and Lamb, E. and Lamprecht, A. and Larkin, D. J. and Laughlin, D. and Le Bagousse-Pinguet, Y. and le Maire, G. and le Roux, P. C. and le Roux, E. and Lee, T. and Lens, F. and Lewis, S. L. and Lhotsky, B. and Li, Y. and Li, X. and Lichstein, J. W. and Liebergesell, M. and Lim, J. Y. and Lin, Y. S. and Linares, J. C. and Liu, C. and Liu, D. and Liu, U. and Livingstone, S. and Llusia, J. and Lohbeck, M. and Lopez-Garcia, A. and Lopez-Gonzalez, G. and Lososova, Z. and Louault, F. and Lukacs, B. A. and Lukes, P. and Luo, Y. and Lussu, M. and Ma, S. and Maciel Rabelo Pereira, C. and Mack, M. and Maire, V. and Makela, A. and Makinen, H. and Malhado, A. C. M. and Mallik, A. and Manning, P. and Manzoni, S. and Marchetti, Z. and Marchino, L. and Marcilio-Silva, V. and Marcon, E. and Marignani, M. and Markesteijn, L. and Martin, A. and Martinez-Garza, C. and Martinez-Vilalta, J. and Maskova, T. and Mason, K. and Mason, N. and Massad, T. J. and Masse, J. and Mayrose, I. and McCarthy, J. and McCormack, M. L. and McCulloh, K. and McFadden, I. R. and McGill, B. J. and McPartland, M. Y. and Medeiros, J. S. and Medlyn, B. and Meerts, P. and Mehrabi, Z. and Meir, P. and Melo, F. P. L. and Mencuccini, M. and Meredieu, C. and Messier, J. and Meszaros, I. and Metsaranta, J. and Michaletz, S. T. and Michelaki, C. and Migalina, S. and Milla, R. and Miller, J. E. D. and Minden, V. and Ming, R. and Mokany, K. and Moles, A. T. and Molnar, A. t. and Molofsky, J. and Molz, M. and Montgomery, R. A. and Monty, A. and Moravcova, L. and Moreno-Martinez, A. and Moretti, M. and Mori, A. S. and Mori, S. and Morris, D. and Morrison, J. and Mucina, L. and Mueller, S. and Muir, C. D. and Muller, S. C. and Munoz, F. and Myers-Smith, I. H. and Myster, R. W. and Nagano, M. and Naidu, S. and Narayanan, A. and Natesan, B. and Negoita, L. and Nelson, A. S. and Neuschulz, E. L. and Ni, J. and Niedrist, G. and Nieto, J. and Niinemets, U. and Nolan, R. and Nottebrock, H. and Nouvellon, Y. and Novakovskiy, A. and Nutrient, N. and Nystuen, K. O. and O'Grady, A. and O'Hara, K. and O'Reilly-Nugent, A. and Oakley, S. and Oberhuber, W. and Ohtsuka, T. and Oliveira, R. and Ollerer, K. and Olson, M. E. and Onipchenko, V. and Onoda, Y. and Onstein, R. E. and Ordonez, J. C. and Osada, N. and Ostonen, I. and Ottaviani, G. and Otto, S. and Overbeck, G. E. and Ozinga, W. A. and Pahl, A. T. and Paine, C. E. T. and Pakeman, R. J. and Papageorgiou, A. C. and Parfionova, E. and Partel, M. and Patacca, M. and Paula, S. and Paule, J. and Pauli, H. and Pausas, J. G. and Peco, B. and Penuelas, J. and Perea, A. and Peri, P. L. and Petisco-Souza, A. C. and Petraglia, A. and Petritan, A. M. and Phillips, O. L. and Pierce, S. and Pillar, V. D. and Pisek, J. and Pomogaybin, A. and Poorter, H. and Portsmuth, A. and Poschlod, P.

and Potvin, C. and Pounds, D. and Powell, A. S. and Power, S. A. and Prinzing, A. and Puglielli, G. and Pysek, P. and Raevel, V. and Rammig, A. and Ransijn, J. and Ray, C. A. and Reich, P. B. and Reichstein, M. and Reid, D. E. B. and Rejou-Mechain, M. and de Dios, V. R. and Ribeiro, S. and Richardson, S. and Riibak, K. and Rillig, M. C. and Riviera, F. and Robert, E. M. R. and Roberts, S. and Robroek, B. and Roddy, A. and Rodrigues, A. V. and Rogers, A. and Rollinson, E. and Rolo, V. and Romermann, C. and Ronzhina, D. and Roscher, C. and Rosell, J. A. and Rosenfield, M. F. and Rossi, C. and Roy, D. B. and Royer-Tardif, S. and Ruger, N. and Ruiz-Peinado, R. and Rumpf, S. B. and Rusch, G. M. and Ryo, M. and Sack, L. and Saldana, A. and Salgado-Negret, B. and Salguero-Gomez, R. and Santa-Regina, I. and Santacruz-Garcia, A. C. and Santos, J. and Sardans, J. and Schamp, B. and Scherer-Lorenzen, M. and Schleuning, M. and Schmid, B. and Schmidt, M. and Schmitt, S. and Schneider, J. V. and Schowanek, S. D. and Schrader, J. and Schrodt, F. and Schuldt, B. and Schurr, F. and Selaya Garvizu, G. and Semchenko, M. and Seymour, C. and Sfair, J. C. and Sharpe, J. M. and Sheppard, C. S. and Sheremetiev, S. and Shiodera, S. and Shipley, B. and Shovon, T. A. and Siebenkas, A. and Sierra, C. and Silva, V. and Silva, M. and Sitzia, T. and Sjoman, H. and Slot, M. and Smith, N. G. and Sodhi, D. and Soltis, P. and Soltis, D. and Somers, B. and Sonnier, G. and Sorensen, M. V. and Sosinski, E. E., Jr. and Soudzilovskaia, N. A. and Souza, A. F. and Spasojevic, M. and Sperandii, M. G. and Stan, A. B. and Stegen, J. and Steinbauer, K. and Stephan, J. G. and Sterck, F. and Stojanovic, D. B. and Strydom, T. and Suarez, M. L. and Svenning, J. C. and Svitkova, I. and Svitok, M. and Svoboda, M. and Swaine, E. and Swenson, N. and Tabarelli, M. and Takagi, K. and Tappeiner, U. and Tarifa, R. and Tauugourdeau, S. and Tavsanoglu, C. and Te Beest, M. and Tedersoo, L. and Thiffault, N. and Thom, D. and Thomas, E. and Thompson, K. and Thornton, P. E. and Thuiller, W. and Tichy, L. and Tissue, D. and Tjoelker, M. G. and Tng, D. Y. P. and Tobias, J. and Torok, P. and Tarin, T. and Torres-Ruiz, J. M. and Tothmeresz, B. and Treurnicht, M. and Trivellone, V. and Trolliet, F. and Trotsiuk, V. and Tsakalos, J. L. and Tsiripidis, I. and Tysklind, N. and Umehara, T. and Usoltsev, V. and Vadeboncoeur, M. and Vaezi, J. and Valladares, F. and Vamosi, J. and van Bodegom, P. M. and van Breugel, M. and Van Cleemput, E. and van de Weg, M. and van der Merwe, S. and van der Plas, F. and van der Sande, M. T. and van Kleunen, M. and Van Meerbeek, K. and Vanderwel, M. and Vanselow, K. A. and Varhammar, A. and Varone, L. and Vasquez Valderrama, M. Y. and Vassilev, K. and Vellend, M. and Veneklaas, E. J. and Verbeeck, H. and Verheyen, K. and Vibrans, A. and Vieira, I. and Villacis, J. and Violle, C. and Vivek, P. and Wagner, K. and Waldram, M. and Waldron, A. and Walker, A. P. and Waller, M. and Walther, G. and Wang, H. and Wang, F. and Wang, W. and Watkins, H. and Watkins, J. and Weber, U. and Weedon, J. T. and Wei, L. and Weigelt, P. and Weiher, E. and Wells, A. W. and Wellstein, C. and Wenk, E. and Westoby, M. and Westwood, A. and White, P. J. and Whitten, M. and Williams, M. and Winkler, D. E. and Winter, K. and Womack, C. and Wright, I. J. and Wright, S. J. and Wright, J. and Pinho, B. X. and Ximenes, F. and Yamada, T. and Yamaji, K. and Yanai, R. and Yankov, N. and Yguel, B. and Zanini, K. J. and Zanne, A. E. and Zeleny, D. and Zhao, Y. P. and Zheng, J. and Zheng, J. and Zieminska, K. and Zirbel, C. R. and Zizka, G. and Zo-Bi, I. C. and Zotz, G. and Wirth, C.: Try Plant Trait Database - Enhanced Coverage and Open Access, Glob Chang Biol, 26, 119-188, https://doi.org/10.1111/gcb.14904, 2020.

Kennedy, R. E., Yang, Z., Gorelick, N., Braaten, J., Cavalcante, L., Cohen, W. B., and Healey, S.: Implementation of the Landtrendr Algorithm on Google Earth Engine, 10, 691, https://doi.org/10.3390/rs10050691, 2018.

Kenzo, T., Ichie, T., Hattori, D., Itioka, T., Handa, C., Ohkubo, T., Kendawang, J. J., Nakamura, M., Sakaguchi, M., Takahashi, N., Okamoto, M., Tanaka-Oda, A., Sakurai, K., and Ninomiya, I.: Development of Allometric Relationships for Accurate Estimation of above- and Below-Ground Biomass in Tropical Secondary Forests in Sarawak, Malaysia, Journal of Tropical Ecology, 25, 371-386, https://doi.org/10.1017/S0266467409006129, 2009.

Ketterings, Q. M., Coe, R., van Noordwijk, M., Ambagau, Y., and Palm, C. A.: Reducing Uncertainty in the Use of Allometric Biomass Equations for Predicting above-Ground Tree Biomass in Mixed Secondary Forests, Forest Ecology and Management, 146, 199-209, https://doi.org/10.1016/S0378-1127(00)00460-6, 2001a.

Ketterings, Q. M., Coe, R., van Noordwijk, M., Ambagau', Y., and Palm, C. A.: Reducing Uncertainty in the Use of Allometric Biomass Equations for Predicting above-Ground Tree Biomass in Mixed Secondary Forests, Forest Ecology and Management, 146, 199-209, https://doi.org/https://doi.org/10.1016/S0378-1127(00)00460-6, 2001b.

Kho, L. K. and Jepsen, M. R.: Carbon Stock of Oil Palm Plantations and Tropical Forests in Malaysia: A Review, Singapore Journal of Tropical Geography, 36, 249-266, https://doi.org/10.1111/sjtg.12100, 2015.

Kim, S., Horn, S., Sok, P., Sien, T., and Yorn, C.: Ecosystem Carbon Stock Assessment in Upland Forest: A Case Study in Koh Kong, Mondulkiri, Preah Vihear, and Siem Reap Provinces, Environmental and Rural Development, 61, 2023.

King, D. A., Davies, S. J., Tan, S., and Noor, N. S. M.: The Role of Wood Density and Stem Support Costs in the Growth and Mortality of Tropical Trees, Journal of Ecology, 94, 670-680, https://doi.org/10.1111/j.1365-2745.2006.01112.x, 2006.

Kiyono, Y., Ito, E., Monda, Y., Toriyama, J., and Sum, T.: Effects of Large Aboveground Biomass Loss Events on the Deadwood and Litter Mass Dynamics of Seasonal Tropical Forests in Cambodia, Tropics, 27, 33-48, https://doi.org/10.3759/tropics.MS18-05, 2018.

Kiyono, Y., Ochiai, Y., Chiba, Y., Asai, H., Saito, K., Shiraiwa, T., Horie, T., Songnoukhai, V., Navongxai, V., and Inoue, Y.: Predicting Chronosequential Changes in Carbon Stocks of Pachymorph Bamboo Communities in Slash-and-Burn Agricultural Fallow, Northern Lao People's Democratic Republic, Journal of Forest Research, 12, 371-383, https://doi.org/10.1007/s10310-007-0028-6, 2007.

Kramer, J. M. F., Zwiener, V. P., and Müller, S. C.: Biotic Homogenization and Differentiation of Plant Communities in Tropical and Subtropical Forests, 37, e14025, https://doi.org/10.1111/cobi.14025, 2023.

Kumaresh, V., Rani, M. S. A., Vethamoni, P. I., Senthil, A., and Uma, D.: Morphological and Physiological Analysis of Vri-3 Cashew Plantations under Different Planting Density Systems, International Journal of Environment and Climate Change, 13, 3698-3706, https://doi.org/10.9734/ijecc/2023/v13i103041, 2023.

Laurance, W. F., Sayer, J., and Cassman, K. G.: Agricultural Expansion and Its Impacts on Tropical Nature, Trends Ecol Evol, 29, 107-116, https://doi.org/10.1016/j.tree.2013.12.001, 2014.

Laurans, M., Hérault, B., Vieilledent, G., and Vincent, G.: Vertical Stratification Reduces Competition for Light in Dense Tropical Forests, Forest Ecology and Management, 329, 79-88, https://doi.org/10.1016/j.foreco.2014.05.059, 2014.

Leoni, E., Altesor, A., and Paruelo, J. M.: Explaining Patterns of Primary Production from Individual Level Traits, Journal of Vegetation Science, 20, 612-619, https://doi.org/10.1111/j.1654-1103.2009.01080.x, 2009.

Lewis, S. L., Sonke, B., Sunderland, T., Begne, S. K., Lopez-Gonzalez, G., van der Heijden, G. M., Phillips, O. L., Affum-Baffoe, K., Baker, T. R., Banin, L., Bastin, J. F., Beeckman, H., Boeckx, P., Bogaert, J., De Canniere, C., Chezeaux, E., Clark, C. J., Collins, M., Djagbletey, G., Djuikouo, M. N., Droissart, V., Doucet, J. L., Ewango, C. E., Fauset, S., Feldpausch, T. R., Foli, E. G., Gillet, J. F., Hamilton, A. C., Harris, D. J., Hart, T. B., de Haulleville, T., Hladik, A., Hufkens, K., Huygens, D., Jeanmart, P., Jeffery, K. J., Kearsley, E., Leal, M. E., Lloyd, J., Lovett, J. C., Makana, J. R., Malhi, Y., Marshall, A. R., Ojo, L., Peh, K. S., Pickavance, G., Poulsen, J. R., Reitsma, J. M., Sheil, D., Simo, M., Steppe, K., Taedoumg, H. E., Talbot, J., Taplin, J. R., Taylor, D., Thomas, S. C., Toirambe, B., Verbeeck, H., Vleminckx, J., White, L. J., Willcock, S., Woell, H., and Zemagho, L.: Above-Ground Biomass and Structure of 260 African Tropical Forests, Philos Trans R Soc Lond B Biol Sci, 368, 20120295, https://doi.org/10.1098/rstb.2012.0295, 2013.

Li, Y., Liu, C., Zhang, J., Yang, H., Xu, L., Wang, Q., Sack, L., Wu, X., Hou, J., and He, N.: Variation in Leaf Chlorophyll Concentration from Tropical to Cold-Temperate Forests: Association with Gross Primary Productivity, Ecological Indicators, 85, 383-389, https://doi.org/10.1016/j.ecolind.2017.10.025, 2018.

Liang, J., Crowther, T. W., Picard, N., Wiser, S., Zhou, M., Alberti, G., Schulze, E. D., McGuire, A. D., Bozzato, F., Pretzsch, H., de-Miguel, S., Paquette, A., Herault, B., Scherer-Lorenzen, M., Barrett, C. B., Glick, H. B., Hengeveld, G. M., Nabuurs, G. J., Pfautsch, S., Viana, H., Vibrans, A. C., Ammer, C., Schall, P., Verbyla, D., Tchebakova, N., Fischer, M., Watson, J. V., Chen, H. Y., Lei, X., Schelhaas, M. J., Lu, H., Gianelle, D., Parfenova, E. I., Salas, C., Lee, E., Lee, B., Kim, H. S., Bruelheide, H., Coomes, D. A., Piotto, D., Sunderland, T., Schmid, B., Gourlet-Fleury, S., Sonke, B., Tavani, R., Zhu, J., Brandl, S., Vayreda, J., Kitahara, F., Searle, E. B., Neldner, V. J., Ngugi, M. R., Baraloto, C., Frizzera, L., Balazy, R., Oleksyn, J., Zawila-Niedzwiecki, T., Bouriaud, O., Bussotti, F., Finer, L., Jaroszewicz, B., Jucker, T., Valladares, F., Jagodzinski, A. M., Peri, P. L., Gonmadje, C., Marthy, W., O'Brien, T., Martin, E. H., Marshall, A. R., Rovero, F., Bitariho, R., Niklaus, P. A., Alvarez-Loayza, P., Chamuya, N., Valencia, R., Mortier, F., Wortel, V., Engone-Obiang, N. L., Ferreira, L. V., Odeke, D. E., Vasquez, R. M., Lewis, S. L., and Reich, P. B.: Positive Biodiversity-Productivity Relationship Predominant in Global Forests, Science, 354, aaf8957-aaf8957, https://doi.org/10.1126/science.aaf8957, 2016.

Liu, Z., Zhao, M., Zhang, H., Ren, T., Liu, C., and He, N.: Divergent Response and Adaptation of Specific Leaf Area to Environmental Change at Different Spatio-Temporal Scales Jointly Improve Plant Survival, Global Change Biology, 29, 1144-1159, https://doi.org/10.1111/gcb.16518, 2023.

Luo, Z., Niu, J., He, S., Zhang, L., Chen, X., Tan, B., Wang, D., and Berndtsson, R.: Linking Roots, Preferential Flow, and Soil Moisture Redistribution in Deciduous and Coniferous Forest Soils, Journal of Soils and Sediments, 23, 1524-1538, https://doi.org/10.1007/s11368-022-03375-w, 2023.

Lutz, J. A., Furniss, T. J., Johnson, D. J., Davies, S. J., Allen, D., Alonso, A., Anderson-Teixeira, K. J., Andrade, A., Baltzer, J., Becker, K. M. L., Blomdahl, E. M., Bourg, N. A., Bunyavejchewin, S., Burslem, D. F. R. P., Cansler, C. A., Cao, K., Cao, M., Cárdenas, D., Chang, L. W., Chao, K. J., Chao, W. C., Chiang, J. M., Chu, C., Chuyong, G. B., Clay, K., Condit, R., Cordell, S., Dattaraja, H. S., Duque, A., Ewango, C. E. N., Fischer, G. A., Fletcher, C., Freund, J. A., Giardina, C., Germain, S. J., Gilbert, G. S., Hao, Z., Hart, T., Hau, B. C. H., He, F., Hector, A., Howe, R. W., Hsieh, C. F., Hu, Y. H., Hubbell, S. P., Inman-Narahari, F. M., Itoh, A., Janík, D., Kassim, A. R., Kenfack, D., Korte, L., Král, K., Larson, A. J., Li, Y., Lin, Y., Liu, S., Lum, S., Ma, K., Makana, J. R., Malhi, Y., McMahon, S. M., McShea, W. J., Memiaghe, H. R., Mi, X., Morecroft, M., Musili, P. M., Myers, J. A., Novotny, V., De Oliveira, A., Ong, P., Orwig, D. A., Ostertag, R., Parker, G. G., Patankar, R., Phillips, R. P., Reynolds, G., Sack, L., Song, G. Z. M., Su, S. H., Sukumar, R., Sun, I. F., Suresh, H. S., Swanson, M. E., Tan, S., Thomas, D. W., Thompson, J., Uriarte, M., Valencia, R., Vicentini, A., Vrška, T., Wang, X., Weiblen, G. D., Wolf, A., Wu, S. H., Xu, H., Yamakura, T., Yap, S., and Zimmerman, J. K.: Global Importance of Large-Diameter Trees, Global Ecology and Biogeography, 27, 849-864, https://doi.org/10.1111/geb.12747, 2018.

Males, J., Artaxo, P., Hansson, H. C., Machado, L. A. T., and Rizzo, L. V.: Tropical Forests Are Crucial in Regulating the Climate on Earth, PLOS Climate, 1, e0000054, https://doi.org/10.1371/journal.pclm.0000054, 2022.

Malimbwi, R. E., Eid, T., and Chamshama, S. A. O.: Allometric Tree Biomass and Volume Models in Tanzania, Sokoine University of Agriculture, Morogoro, Tanzania https://doi.org/10.13140/RG.2.1.1891.5445, 2016.

Manuel Villa, P., Ali, A., Venâncio Martins, S., Nolasco de Oliveira Neto, S., Cristina Rodrigues, A., Teshome, M., Alvim Carvalho, F., Heringer, G., and Gastauer, M.: Stand Structural Attributes and Functional Trait Composition Overrule the Effects of Functional Divergence on Aboveground Biomass during Amazon Forest Succession, Forest Ecology and Management, 477, 118481, https://doi.org/https://doi.org/10.1016/j.foreco.2020.118481, 2020.

Maréchaux, I., Bonal, D., Bartlett, M. K., Burban, B., Coste, S., Courtois, E. A., Dulormne, M., Goret, J.-Y., Mira, E., Mirabel, A., Sack, L., Stahl, C., and Chave, J.: Dry-Season Decline in Tree Sapflux Is Correlated with Leaf Turgor Loss Point in a Tropical Rainforest, 32, 2285-2297, https://doi.org/10.1111/1365-2435.13188, 2018.

Matschullat, J.: Save Cambodia’s Wildlife: Atlas of Cambodia. Maps on Socio-Economic Development and Environment, Environmental Earth Sciences, 72, 1295-1298, https://doi.org/10.1007/s12665-014-3325-3, 2014.

Miettinen, J., Shi, C. H., and Liew, S. C.: Deforestation Rates in Insular Southeast Asia between 2000 and 2010, Global Change Biology, 17, 2261-2270, https://doi.org/10.1111/j.1365-2486.2011.02398.x, 2011.

Mlagalila, H. E.: Assessment of Volume, Biomass and Carbon Stock of Cashewnuts Trees in Liwale District, Tanzania, 2016.

Mog, B. and Nayak, M. G.: Leaf Morphological and Physiological Traits and Their Significance in Yield Improvement of Fifteen Cashew Varieties in West Coast Region of Karnataka, International Journal of Current Microbiology and Applied Sciences, 7, 1455-1469, https://doi.org/10.20546/ijcmas.2018.707.173, 2018.

Mohd Nazip, S.: Tree Species Diversity and Forest Stand Structure of Pahang National Park, Malaysia, in: Biodiversity Enrichment in a Diverse World, edited by: Gbolagade Akeem, L., IntechOpen, Rijeka, Ch. 18, https://doi.org/10.5772/50339, 2012.

Mrad, A., Manzoni, S., Oren, R., Vico, G., Lindh, M., and Katul, G.: Recovering the Metabolic, Self-Thinning, and Constant Final Yield Rules in Mono-Specific Stands, 3, https://doi.org/10.3389/ffgc.2020.00062, 2020.

Naeem, S., Thompson, L. J., Lawler, S. P., Lawton, J. H., and Woodfin, R. M.: Declining Biodiversity Can Alter the Performance of Ecosystems, Nature, 368, 734-737, https://doi.org/10.1038/368734a0, 1994.

Ndiaye, S., Djighaly, P. I., Diarra, A., and Dramé, F. A.: Comparative Study of the Carbon Stock of a Cashew Tree Plantation (Anacardium Occidentale L.) and Secondary Forest in Casamance, Senegal, Nguyen, T. D. and Kappas, M.: Estimating the Aboveground Biomass of an Evergreen Broadleaf Forest in Xuan Lien Nature Reserve, Thanh Hoa, Vietnam, Using Spot-6 Data and the Random Forest Algorithm, International Journal of Forestry Research, 2020, 1-13, https://doi.org/10.1155/2020/4216160, 2020.

Niinemets, Ü.: A Review of Light Interception in Plant Stands from Leaf to Canopy in Different Plant Functional Types and in Species with Varying Shade Tolerance, Ecological Research, 25, 693-714, https://doi.org/10.1007/s11284-010-0712-4, 2010.

Nyirambangutse, B., Zibera, E., Uwizeye, F. K., Nsabimana, D., Bizuru, E., Pleijel, H., Uddling, J., and Wallin, G.: Carbon Stocks and Dynamics at Different Successional Stages in an Afromontane Tropical Forest, Biogeosciences, 14, 1285-1303, https://doi.org/10.5194/bg-14-1285-2017, 2017.

Nzegbule, E. C., Onyema, M. C., Ndelekwute, S. C., and State, A.: Plant Species Richness and Soil Nutrients in a 35-Year Old Cashew Nut Plantation in Isuochi, Southern Nigeria,

Olofsson, P. and Eklundh, L.: Estimation of Absorbed Par across Scandinavia from Satellite Measurements. Part Ii: Modeling and Evaluating the Fractional Absorption, Remote Sensing of Environment, 110, 240-251, https://doi.org/10.1016/j.rse.2007.02.020, 2007.

Omuto, C. T., Vargas, R., Viatkin, K., and Yigini, Y. (Eds.): Lesson 4 – Spatial Modeling of Salt-Affected Soils, Global Soil Salinity Map – Gssmap, FAO, Room, Italy, 2020.

Ota, T., Ogawa, M., Shimizu, K., Kajisa, T., Mizoue, N., Yoshida, S., Takao, G., Hirata, Y., Furuya, N., Sano, T., Sokh, H., Ma, V., Ito, E., Toriyama, J., Monda, Y., Saito, H., Kiyono, Y., Chann, S., and Ket, N.: Aboveground Biomass Estimation Using Structure from Motion Approach with Aerial Photographs in a Seasonal Tropical Forest, Forests, 6, 3882-3898, https://doi.org/10.3390/f6113882, 2015.

Pan, Y., Birdsey, R. A., Phillips, O. L., Houghton, R. A., Fang, J., Kauppi, P. E., Keith, H., Kurz, W. A., Ito, A., Lewis, S. L., Nabuurs, G.-J., Shvidenko, A., Hashimoto, S., Lerink, B., Schepaschenko, D., Castanho, A., and Murdiyarso, D.: The Enduring World Forest Carbon Sink, Nature, 631, 563-569, https://doi.org/10.1038/s41586-024-07602-x, 2024.

Parisi, F., Pioli, S., Lombardi, F., Fravolini, G., Marchetti, M., and Tognetti, R.: Linking Deadwood Traits with Saproxylic Invertebrates and Fungi in European Forests - a Review, 11, 423-436, https://doi.org/10.3832/ifor2670-011, 2018a.

Parisi, F., Pioli, S., Lombardi, F., Fravolini, G., Marchetti, M., and Tognetti, R.: Linking Deadwood Traits with Saproxylic Invertebrates and Fungi in European Forests - a Review, Iforest-Biogeosciences and Forestry, 11, 423-436, https://doi.org/10.3832/ifor2670-011, 2018b.

Pastorello, G., Trotta, C., Canfora, E., Chu, H., Christianson, D., Cheah, Y. W., Poindexter, C., Chen, J., Elbashandy, A., Humphrey, M., Isaac, P., Polidori, D., Reichstein, M., Ribeca, A., van Ingen, C., Vuichard, N., Zhang, L., Amiro, B., Ammann, C., Arain, M. A., Ardo, J., Arkebauer, T., Arndt, S. K., Arriga, N., Aubinet, M., Aurela, M., Baldocchi, D., Barr, A., Beamesderfer, E., Marchesini, L. B., Bergeron, O., Beringer, J., Bernhofer, C., Berveiller, D., Billesbach, D., Black, T. A., Blanken, P. D., Bohrer, G., Boike, J., Bolstad, P. V., Bonal, D., Bonnefond, J. M., Bowling, D. R., Bracho, R., Brodeur, J., Brummer, C., Buchmann, N., Burban, B., Burns, S. P., Buysse, P., Cale, P., Cavagna, M., Cellier, P., Chen, S., Chini, I., Christensen, T. R., Cleverly, J., Collalti, A., Consalvo, C., Cook, B. D., Cook, D., Coursolle, C., Cremonese, E., Curtis, P. S., D'Andrea, E., da Rocha, H., Dai, X., Davis, K. J., Cinti, B., Grandcourt, A., Ligne, A., De Oliveira, R. C., Delpierre, N., Desai, A. R., Di Bella, C. M., Tommasi, P. D., Dolman, H., Domingo, F., Dong, G., Dore, S., Duce, P., Dufrene, E., Dunn, A., Dusek, J., Eamus, D., Eichelmann, U., ElKhidir, H. A. M., Eugster, W., Ewenz, C. M., Ewers, B., Famulari, D., Fares, S., Feigenwinter, I., Feitz, A., Fensholt, R., Filippa, G., Fischer, M., Frank, J., Galvagno, M., Gharun, M., Gianelle, D., Gielen, B., Gioli, B., Gitelson, A., Goded, I., Goeckede, M., Goldstein, A. H., Gough, C. M., Goulden, M. L., Graf, A., Griebel, A., Gruening, C., Grunwald, T., Hammerle, A., Han, S., Han, X., Hansen, B. U., Hanson, C., Hatakka, J., He, Y., Hehn, M., Heinesch, B., Hinko-Najera, N., Hortnagl, L., Hutley, L., Ibrom, A., Ikawa, H., Jackowicz-Korczynski, M., Janous, D., Jans, W., Jassal, R., Jiang, S., Kato, T., Khomik, M., Klatt, J., Knohl, A., Knox, S., Kobayashi, H., Koerber, G., Kolle, O., Kosugi, Y., Kotani, A., Kowalski, A., Kruijt, B., Kurbatova, J., Kutsch, W. L., Kwon, H., Launiainen, S., Laurila, T., Law, B., Leuning, R., Li, Y., Liddell, M., Limousin, J. M., Lion, M., Liska, A. J., Lohila, A., Lopez-Ballesteros, A., Lopez-Blanco, E., Loubet, B., Loustau, D., Lucas-Moffat, A., Luers, J., Ma, S., Macfarlane, C., Magliulo, V., Maier, R., Mammarella, I., Manca, G., Marcolla, B., Margolis, H. A., Marras, S., Massman, W., Mastepanov, M., Matamala, R., Matthes, J. H., Mazzenga, F., McCaughey, H., McHugh, I., McMillan, A. M. S., Merbold, L., Meyer, W., Meyers, T., Miller, S. D., Minerbi, S., Moderow, U., Monson, R. K., Montagnani, L., Moore, C. E., Moors, E., Moreaux, V., Moureaux, C., Munger, J. W., Nakai, T., Neirynck, J., Nesic, Z., Nicolini, G., Noormets, A., Northwood, M., Nosetto, M., Nouvellon, Y., Novick, K., Oechel, W., Olesen, J. E., Ourcival, J. M., Papuga, S. A., Parmentier, F. J., Paul-Limoges, E., Pavelka, M., Peichl, M., Pendall, E., Phillips, R. P., Pilegaard, K., Pirk, N., Posse, G., Powell, T., Prasse, H., Prober, S. M., Rambal, S., Rannik, U., Raz-Yaseef, N., Rebmann, C., Reed, D., Dios, V. R., Restrepo-Coupe, N., Reverter, B. R., Roland, M., Sabbatini, S., Sachs, T., Saleska, S. R., Sanchez-Canete, E. P., Sanchez-Mejia, Z. M., Schmid, H. P., Schmidt, M., Schneider, K., Schrader, F., Schroder, I., Scott, R. L., Sedlak, P., Serrano-Ortiz, P., Shao, C., Shi, P., Shironya, I., Siebicke, L., Sigut, L., Silberstein, R., Sirca, C., Spano, D., Steinbrecher, R., Stevens, R. M., Sturtevant, C., Suyker, A., Tagesson, T., Takanashi, S., Tang, Y., Tapper, N., Thom, J., Tomassucci, M., Tuovinen, J. P., Urbanski, S., Valentini, R., van der Molen, M., van Gorsel, E., van Huissteden, K., Varlagin, A., Verfaillie, J., Vesala, T., Vincke, C., Vitale, D., Vygodskaya, N., Walker, J. P., Walter-Shea, E., Wang, H., Weber, R., Westermann, S., Wille, C., Wofsy, S., Wohlfahrt, G., Wolf, S., Woodgate, W., Li, Y., Zampedri, R., Zhang, J., Zhou, G., Zona, D., Agarwal, D., Biraud, S., Torn, M., and Papale, D.: The Fluxnet2015 Dataset and the Oneflux Processing Pipeline for Eddy Covariance Data, Sci Data, 7, 225, https://doi.org/10.1038/s41597-020-0534-3, 2020.

Pearson, T. R. H., Brown, S., Murray, L., and Sidman, G.: Greenhouse Gas Emissions from Tropical Forest Degradation: An Underestimated Source, Carbon Balance Manag, 12, 3, https://doi.org/10.1186/s13021-017-0072-2, 2017.

Pei, Y., Dong, J., Zhang, Y., Yuan, W., Doughty, R., Yang, J., Zhou, D., Zhang, L., and Xiao, X.: Evolution of Light Use Efficiency Models: Improvement, Uncertainties, and Implications, Agricultural and Forest Meteorology, 317, 108905, https://doi.org/https://doi.org/10.1016/j.agrformet.2022.108905, 2022.

Phompila, C., Lewis, M., Clarke, K., and Ostendorf, B.: Monitoring Expansion of Plantations in Lao Tropical Forests Using Landsat Time Series, Land Surface Remote Sensing II, 296-306, https://doi.org/10.1117/12.2068283, 2014.

Pickering, B. J., Duff, T. J., Baillie, C., and Cawson, J. G.: Darker, Cooler, Wetter: Forest Understories Influence Surface Fuel Moisture, Agricultural and Forest Meteorology, 300, 108311, https://doi.org/10.1016/j.agrformet.2020.108311, 2021.

Poorter, L.: Functional Recovery of Secondary Tropical Forests (V1), DANS Data Station Life Sciences [dataset], https://doi.org/doi:10.17026/dans-zz5-hf3s, 2021.

R Core Team: R: A Language and Environment for Statistical Computing. R Foundation for Statistical Computing. Vienna. Austria, 2023.

Rawat, M., Arunachalam, K., Arunachalam, A., Alatalo, J. M., and Pandey, R.: Assessment of Leaf Morphological, Physiological, Chemical and Stoichiometry Functional Traits for Understanding the Functioning of Himalayan Temperate Forest Ecosystem, Scientific Reports, 11, https://doi.org/10.1038/s41598-021-03235-6, 2021.

Reich, P. B., Uhl, C., Walters, M. B., and Ellsworth, D. S.: Leaf Lifespan as a Determinant of Leaf Structure and Function among 23 Amazonian Tree Species, Oecologia, 86, 16-24, https://doi.org/10.1007/BF00317383, 1991.

Reyes, G., Brown, S., Chapman, J., and Lugo, A. E.: Wood Densities of Tropical Tree Species, U.S. Department of Agriculture, Forest Service, Southern Forest Experiment Station, https://doi.org/10.2737/so-gtr-88, 1992.

Rodell, M., Houser, P. R., Jambor, U., Gottschalck, J., Mitchell, K., Meng, C. J., Arsenault, K., Cosgrove, B., Radakovich, J., Bosilovich, M., Entin, J. K., Walker, J. P., Lohmann, D., and Toll, D.: The Global Land Data Assimilation System, Bulletin of the American Meteorological Society, 85, 381-394, https://doi.org/10.1175/BAMS-85-3-381, 2004.

Román-Dañobeytia, F. J., Levy-Tacher, S. I., Macario-Mendoza, P., and Zúñiga-Morales, J.: Redefining Secondary Forests in the Mexican Forest Code: Implications for Management, Restoration, and Conservation, 5, 978-991, 2014.

Rosa, M., Rubio Neto, A., Marques, V. d. O., Silva, F. G., de Assis, E. S., Costa, A. C., Dantas, L. A., and Pereira, P. S.: Variations in Photon Flux Density Alter the Morphophysiological and Chemical Characteristics of Anacardium Othonianum Rizz. In Vitro, Plant Cell, Tissue and Organ Culture (PCTOC), 140, 523-537, https://doi.org/10.1007/s11240-019-01744-x, 2020.

Rundel, P. W.: Forest Habitats and Flora in Lao Pdr, Cambodia, and Vietnam, Hanoi: WWF Indochina Programme, 1999.

Saner, P., Loh, Y. Y., Ong, R. C., and Hector, A.: Carbon Stocks and Fluxes in Tropical Lowland Dipterocarp Rainforests in Sabah, Malaysian Borneo, PLOS ONE, 7, e29642, https://doi.org/10.1371/journal.pone.0029642, 2012.

Santopuoli, G., Temperli, C., Alberdi, I., Barbeito, I., Bosela, M., Bottero, A., Klopčič, M., Lesinski, J., Panzacchi, P., and Tognetti, R.: Pan-European Sustainable Forest Management Indicators for Assessing Climate-Smart Forestry in Europe, 51, 1741-1750, https://doi.org/10.1139/cjfr-2020-0166, 2021.

Schindelin, J., Arganda-Carreras, I., Frise, E., Kaynig, V., Longair, M., Pietzsch, T., Preibisch, S., Rueden, C., Saalfeld, S., Schmid, B., Tinevez, J. Y., White, D. J., Hartenstein, V., Eliceiri, K., Tomancak, P., and Cardona, A.: Fiji: An Open-Source Platform for Biological-Image Analysis, Nat Methods, 9, 676-682, https://doi.org/10.1038/nmeth.2019, 2012.

Schneider, C. A., Rasband, W. S., and Eliceiri, K. W.: Nih Image to Imagej: 25 Years of Image Analysis, Nat Methods, 9, 671-675, https://doi.org/10.1038/nmeth.2089, 2012.

Senf, C., Mori, A. S., Müller, J., and Seidl, R.: The Response of Canopy Height Diversity to Natural Disturbances in Two Temperate Forest Landscapes, Landscape Ecology, 35, 2101-2112, https://doi.org/10.1007/s10980-020-01085-7, 2020.

Senior, R. A., Hill, J. K., Benedick, S., and Edwards, D. P.: Tropical Forests Are Thermally Buffered Despite Intensive Selective Logging, 24, 1267-1278, https://doi.org/10.1111/gcb.13914, 2018.

Senna, M. C. A., Costa, M. H., and Shimabukuro, Y. E.: Fraction of Photosynthetically Active Radiation Absorbed by Amazon Tropical Forest: A Comparison of Field Measurements, Modeling, and Remote Sensing, 110, https://doi.org/10.1029/2004JG000005, 2005.

Shannon, C. E.: A Mathematical Theory of Communication, Bell System Technical Journal, 27, 379-423, https://doi.org/10.1002/j.1538-7305.1948.tb01338.x, 1948.

Shannon, V. L., Vanguelova, E. I., Morison, J. I. L., Shaw, L. J., and Clark, J. M.: The Contribution of Deadwood to Soil Carbon Dynamics in Contrasting Temperate Forest Ecosystems, European Journal of Forest Research, 141, 241-252, https://doi.org/10.1007/s10342-021-01435-3, 2021.

Slik, J. W. F., Aiba, S. I., Brearley, F. Q., Cannon, C. H., Forshed, O., Kitayama, K., Nagamasu, H., Nilus, R., Payne, J., Paoli, G., Poulsen, A. D., Raes, N., Sheil, D., Sidiyasa, K., Suzuki, E., and van Valkenburg, J. L. C. H.: Environmental Correlates of Tree Biomass, Basal Area, Wood Specific Gravity and Stem Density Gradients in Borneo's Tropical Forests, Global Ecology and Biogeography, 19, 50-60, https://doi.org/10.1111/j.1466-8238.2009.00489.x, 2010.

Sodhi, N. S., Koh, L. P., Brook, B. W., and Ng, P. K.: Southeast Asian Biodiversity: An Impending Disaster, Trends Ecol Evol, 19, 654-660, https://doi.org/10.1016/j.tree.2004.09.006, 2004.

Somaly, O., Sasaki, N., Kimchhin, S., Tsusaka, T. W., Shrestha, S., and Malyne, N.: Impact of Forest Cover Change in Phnom Kulen National Park on Downstream Local Livelihoods Along Siem Reap River, Cambodia, International Journal of Environmental and Rural Development, 11, 93-99, https://doi.org/10.32115/ijerd.11.1_93, 2020.

Sovann, C., Tagesson, T., Kok, S., and Olin, S.: Forest Inventory, Leaf Area Index, and Leaf Functional Traits of Various Land Cover Classes in Kulen, Cambodia, Zenodo [dataset], https://doi.org/10.5281/zenodo.10146582, 2024a.

Sovann, C., Tagesson, T., Vestin, P., Kok, S., and Olin, S.: Daily Fraction of Photosynthetically Active Radiation (Fpar), Edaphic, and Weather Conditions from 20220410 to 20230409 in Kulen, Cambodia, Zenodo [dataset], https://doi.org/10.5281/zenodo.10159726, 2024b.

Sovann, C., Olin, S., Mansourian, A., Sakhoeun, S., Prey, S., Kok, S., and Tagesson, T.: Importance of Spectral Information, Seasonality, and Topography on Land Cover Classification of Tropical Land Cover Mapping, https://doi.org/10.3390/rs17091551, 2025.

Sovu, Tigabu, M., Savadogo, P., Odén, P. C., and Xayvongsa, L.: Recovery of Secondary Forests on Swidden Cultivation Fallows in Laos, Forest Ecology and Management, 258, 2666-2675, https://doi.org/10.1016/j.foreco.2009.09.030, 2009.

Steur, G., Ter Steege, H., Verburg, R. W., Sabatier, D., Molino, J. F., Banki, O. S., Castellanos, H., Stropp, J., Fonty, E., Ruysschaert, S., Galbraith, D., Kalamandeen, M., van Andel, T. R., Brienen, R., Phillips, O. L., Feeley, K. J., Terborgh, J., and Verweij, P. A.: Relationships between Species Richness and Ecosystem Services in Amazonian Forests Strongly Influenced by Biogeographical Strata and Forest Types, Sci Rep, 12, 5960, https://doi.org/10.1038/s41598-022-09786-6, 2022.

Stibig, H. J., Achard, F., Carboni, S., Rasi, R., and Miettinen, J.: Change in Tropical Forest Cover of Southeast Asia from 1990 to 2010, Biogeosciences, 11, 247-258, https://doi.org/10.5194/bg-11-247-2014, 2014.

Stirbet, A., Lazár, D., Guo, Y., and Govindjee, G.: Photosynthesis: Basics, History and Modelling, Annals of Botany, 126, 511-537, https://doi.org/10.1093/aob/mcz171, 2020.

Swedish NFI: Swedish National Forest Inventory and Swedish Soil Inventory: Field Work Instructions 2019, The Department of Forest Resource Management. Swedish University of Agricultural Sciences, Umeå, Sweden, 504, 2019.

Tang, C., Liu, Y., Li, Z., Guo, L., Xu, A., and Zhao, J.: Effectiveness of Vegetation Cover Pattern on Regulating Soil Erosion and Runoff Generation in Red Soil Environment, Southern China, Ecological Indicators, 129, 107956, https://doi.org/10.1016/j.ecolind.2021.107956, 2021.

ter Steege, H., Pitman, N. C. A., do Amaral, I. L., de Souza Coelho, L., de Almeida Matos, F. D., de Andrade Lima Filho, D., Salomão, R. P., Wittmann, F., Castilho, C. V., Guevara, J. E., Veiga Carim, M. d. J., Phillips, O. L., Magnusson, W. E., Sabatier, D., Revilla, J. D. C., Molino, J.-F., Irume, M. V., Martins, M. P., da Silva Guimarães, J. R., Ramos, J. F., Bánki, O. S., Piedade, M. T. F., Cárdenas López, D., Rodrigues, D. d. J., Demarchi, L. O., Schöngart, J., Almeida, E. J., Barbosa, L. F., Cavalheiro, L., dos Santos, M. C. V., Luize, B. G., de Leão Novo, E. M. M., Vargas, P. N., Silva, T. S. F., Venticinque, E. M., Manzatto, A. G., Reis, N. F. C., Terborgh, J., Casula, K. R., Honorio Coronado, E. N., Monteagudo Mendoza, A., Montero, J. C., Costa, F. R. C., Feldpausch, T. R., Quaresma, A. C., Castaño Arboleda, N., Zartman, C. E., Killeen, T. J., Marimon, B. S., Marimon-Junior, B. H., Vasquez, R., Mostacedo, B., Assis, R. L., Baraloto, C., do Amaral, D. D., Engel, J., Petronelli, P., Castellanos, H., de Medeiros, M. B., Simon, M. F., Andrade, A., Camargo, J. L., Laurance, W. F., Laurance, S. G. W., Maniguaje Rincón, L., Schietti, J., Sousa, T. R., de Sousa Farias, E., Lopes, M. A., Magalhães, J. L. L., Nascimento, H. E. M., de Queiroz, H. L., Aymard C, G. A., Brienen, R., Stevenson, P. R., Araujo-Murakami, A., Baker, T. R., Cintra, B. B. L., Feitosa, Y. O., Mogollón, H. F., Duivenvoorden, J. F., Peres, C. A., Silman, M. R., Ferreira, L. V., Lozada, J. R., Comiskey, J. A., Draper, F. C., de Toledo, J. J., Damasco, G., García-Villacorta, R., Lopes, A., Vicentini, A., Cornejo Valverde, F., Alonso, A., Arroyo, L., Dallmeier, F., Gomes, V. H. F., Jimenez, E. M., Neill, D., Peñuela Mora, M. C., Noronha, J. C., de Aguiar, D. P. P., Barbosa, F. R., Bredin, Y. K., de Sá Carpanedo, R., Carvalho, F. A., de Souza, F. C., Feeley, K. J., Gribel, R., Haugaasen, T., Hawes, J. E., Pansonato, M. P., Ríos Paredes, M., Barlow, J., Berenguer, E., da Silva, I. B., Ferreira, M. J., Ferreira, J., Fine, P. V. A., Guedes, M. C., Levis, C., Licona, J. C., Villa Zegarra, B. E., Vos, V. A., Cerón, C., Durgante, F. M., Fonty, É., Henkel, T. W., Householder, J. E., Huamantupa-Chuquimaco, I., Pos, E., Silveira, M., Stropp, J., Thomas, R., Daly, D., Dexter, K. G., Milliken, W., Molina, G. P., Pennington, T., Vieira, I. C. G., Weiss Albuquerque, B., Campelo, W., Fuentes, A., Klitgaard, B., Pena, J. L. M., Tello, J. S., Vriesendorp, C., Chave, J., Di Fiore, A., Hilário, R. R., de Oliveira Pereira, L., Phillips, J. F., Rivas-Torres, G., van Andel, T. R., von Hildebrand, P., Balee, W., Barbosa, E. M., de Matos Bonates, L. C., Dávila Doza, H. P., Zárate Gómez, R., Gonzales, T., Gallardo Gonzales, G. P., Hoffman, B., Junqueira, A. B., Malhi, Y., de Andrade Miranda, I. P., Pinto, L. F. M., Prieto, A., Rudas, A., Ruschel, A. R., Silva, N., Vela, C. I. A., Zent, E. L., Zent, S., Cano, A., Carrero Márquez, Y. A., Correa, D. F., Costa, J. B. P., Flores, B. M., Galbraith, D., Holmgren, M., Kalamandeen, M., Lobo, G., Torres Montenegro, L., Nascimento, M. T., Oliveira, A. A., Pombo, M. M., Ramirez-Angulo, H., Rocha, M., Scudeller, V. V., Sierra, R., Tirado, M., Umaña, M. N., van der Heijden, G., Vilanova Torre, E., Reategui, M. A. A., Baider, C., Balslev, H., Cárdenas, S., Casas, L. F., Endara, M. J., Farfan-Rios, W., Ferreira, C., Linares-Palomino, R., Mendoza, C., Mesones, I., Parada, G. A., Torres-Lezama, A., Urrego Giraldo, L. E., Villarroel, D., Zagt, R., Alexiades, M. N., de Oliveira, E. A., Garcia-Cabrera, K., Hernandez, L., Cuenca, W. P., Pansini, S., Pauletto, D., Ramirez Arevalo, F., Sampaio, A. F., Valderrama Sandoval, E. H., Gamarra, L. V., Levesley, A., Pickavance, G., and Melgaço, K.: Mapping Density, Diversity and Species-Richness of the Amazon Tree Flora, Communications Biology, 6, 1130, https://doi.org/10.1038/s42003-023-05514-6, 2023.

Than, S., Vesa, L., Vanna, S., Hyvönen, P., Korhonen, K., Gael, S., Matieu, H., and van Rijn, M.: Field Manual for the National Forest Inventory of Cambodia, 2nd Eds, Forest Administration of the Ministry of Agriculture, Forestry and Fisheries & Food and Agriculture Organization of the United Nations, Phnom Penh, Cambodia, 2018.

Theilade, I., Phourin, C., Schmidt, L., Meilby, H., Van De Bult, M., and Friborg, K. G.: Evergreen Forest Types of the Central Plains in Cambodia: Floristic Composition and Ecological Characteristics, Nordic Journal of Botany, 2022, https://doi.org/10.1111/njb.03494, 2022.

Thiel, S., Tschapka, M., Heymann, E. W., and Heer, K.: Vertical Stratification of Seed-Dispersing Vertebrate Communities and Their Interactions with Plants in Tropical Forests, 96, 454-469, https://doi.org/10.1111/brv.12664, 2021.

Tilman, D., Lehman, C. L., and Thomson, K. T.: Plant Diversity and Ecosystem Productivity: Theoretical Considerations, Proc Natl Acad Sci U S A, 94, 1857-1861, https://doi.org/10.1073/pnas.94.5.1857, 1997.

Tito, R., Salinas, N., Cosio, E. G., Espinoza, T. E. B., Muñiz, J. G., Aragón, S., Nina, A., and Roman-Cuesta, R. M.: Secondary Forests in Peru: Differential Provision of Ecosystem Services Compared to Other Post-Deforestation Forest Transitions, Ecology and Society, 27, https://doi.org/10.5751/Es-13446-270312, 2022.

Tláskal, V., Brabcová, V., Větrovský, T., Jomura, M., López-Mondéjar, R., Monteiro, L. M. O., Saraiva, J. P., Human, Z. R., Cajthaml, T., Rocha, U. N. d., and Baldrian, P.: Complementary Roles of Wood-Inhabiting Fungi and Bacteria Facilitate Deadwood Decomposition, 6, 10.1128/msystems.01078-01020, https://doi.org/doi:10.1128/msystems.01078-20, 2021.

Townsend, A. R., Cleveland, C. C., Houlton, B. Z., Alden, C. B., and White, J. W. C.: Multi-Element Regulation of the Tropical Forest Carbon Cycle, Frontiers in Ecology and the Environment, 9, 9-17, https://doi.org/10.1890/100047, 2011.

Tynsong, H., Dkhar, M., and Tiwari, B. K.: Tree Diversity and Vegetation Structure of the Tropical Evergreen Forests of the Southern Slopes of Meghalaya, North East India, Asian Journal of Forestry, 6, https://doi.org/10.13057/asianjfor/r060104, 2022.

Van Do, T., Yamamoto, M., Kozan, O., Hai, V. D., Trung, P. D., Thang, N. T., Hai, L. T., Nam, V. T., Hung, T. T., Van Thang, H., Manh, T. D., Khiem, C. C., Lam, V. T., Hung, N. Q., Quy, T. H., Tuyen, P. Q., Bon, T. N., Phuong, N. T. T., Khuong, N. V., Van Tuan, N., Ha, D. T. H., Long, T. H., Van Thuyet, D., Trieu, D. T., Van Thinh, N., Hai, T. A., Trung, D. Q., Van Bich, N., Dang, D. H., Dung, P. T., Hoang, N. H., Hanh, L. T., Quang, P. M., Huong, N. T. T., Son, H. T., Son, N. T., Van Anh, N. T., Anh, N. T. H., Sam, P. D., Nhung, H. T., Van Thanh, H., Thinh, N. H., Van, T. H., Luong, H. T., and Hung, B. K.: Ecoregional Variations of Aboveground Biomass and Stand Structure in Evergreen Broadleaved Forests, Journal of Forestry Research, 31, 1713-1722, https://doi.org/10.1007/s11676-019-00969-y, 2019.

van Galen, L. G., Jordan, G. J., and Baker, S. C.: Relationships between Coarse Woody Debris Habitat Quality and Forest Maturity Attributes, 1, e55, https://doi.org/10.1111/csp2.55, 2019.

van Haren, J., de Oliveira Jr, R. C., Beldini, P. T., de Camargo, P. B., Keller, M., and Saleska, S.: Tree Species Effects on Soil Properties and Greenhouse Gas Fluxes in East-Central Amazonia: Comparison between Monoculture and Diverse Forest, 45, 709-718, https://doi.org/10.1111/btp.12061, 2013.

Van, Y. T. and Cochard, R.: Tree Species Diversity and Utilities in a Contracting Lowland Hillside Rainforest Fragment in Central Vietnam, Forest Ecosystems, 4, 9, https://doi.org/10.1186/s40663-017-0095-x, 2017.

Vestin, P., Mölder, M., Kljun, N., Cai, Z., Hasan, A., Holst, J., Klemedtsson, L., and Lindroth, A.: Impacts of Clear-Cutting of a Boreal Forest on Carbon Dioxide, Methane and Nitrous Oxide Fluxes, https://doi.org/10.3390/f11090961, 2020.

Victor, A. D., Valery, N. N., Boris, N., Aimé, V. B. T., and Louis, Z.: Carbon Storage in Cashew Plantations in Central Africa: Case of Cameroon, Carbon Management, 12, 25-35, https://doi.org/10.1080/17583004.2020.1858682, 2021.

Vieilledent, G., Vaudry, R., Andriamanohisoa, S. F. D., Rakotonarivo, O. S., Randrianasolo, H. Z., Razafindrabe, H. N., Rakotoarivony, C. B., Ebeling, J., and Rasamoelina, M.: A Universal Approach to Estimate Biomass and Carbon Stock in Tropical Forests Using Generic Allometric Models, Ecological Applications, 22, 572-583, https://doi.org/https://doi.org/10.1890/11-0039.1, 2012.

Waide, R. B., Willig, M. R., Steiner, C. F., Mittelbach, G., Gough, L., Dodson, S. I., Juday, G. P., and Parmenter, R.: The Relationship between Productivity and Species Richness, Annual Review of Ecology and Systematics, 30, 257-300, https://doi.org/10.1146/annurev.ecolsys.30.1.257, 1999.

Wang, P., Li, R., Liu, D., and Wu, Y.: Dynamic Characteristics and Responses of Ecosystem Services under Land Use/Land Cover Change Scenarios in the Huangshui River Basin, China, Ecological Indicators, 144, 109539, https://doi.org/https://doi.org/10.1016/j.ecolind.2022.109539, 2022.

Wang, R., Yu, G., He, N., Wang, Q., Zhao, N., and Xu, Z.: Latitudinal Variation of Leaf Morphological Traits from Species to Communities Along a Forest Transect in Eastern China, Journal of Geographical Sciences, 26, 15-26, https://doi.org/10.1007/s11442-016-1251-x, 2016.

Wang, S., Fu, B. J., Gao, G. Y., Yao, X. L., and Zhou, J.: Soil Moisture and Evapotranspiration of Different Land Cover Types in the Loess Plateau, China, Hydrol. Earth Syst. Sci., 16, 2883-2892, https://doi.org/10.5194/hess-16-2883-2012, 2012.

Wang, W., Liu, H. M., Zhang, J. H., Li, Z. Y., Wang, L. X., Wang, Z., Wu, Y. T., Wang, Y., and Liang, C. Z.: Effect of Grazing Types on Community-Weighted Mean Functional Traits and Ecosystem Functions on Inner Mongolian Steppe, China, Sustainability, 12, 7169, https://doi.org/10.3390/su12177169, 2020.

West, G. B. and Brown, J. H.: The Origin of Allometric Scaling Laws in Biology from Genomes to Ecosystems: Towards a Quantitative Unifying Theory of Biological Structure and Organization, J Exp Biol, 208, 1575-1592, https://doi.org/10.1242/jeb.01589, 2005.

Whitmore, T. C.: An Introduction to Tropical Forests, 2nd ed, Oxford University Press Oxford, England, Oxford, England1998.

Woodall, C. W., Evans, D. M., Fraver, S., Green, M. B., Lutz, D. A., and D'Amato, A. W.: Real-Time Monitoring of Deadwood Moisture in Forests: Lessons Learned from an Intensive Case Study, Canadian Journal of Forest Research, 50, 1244-1252, https://doi.org/10.1139/cjfr-2020-0110, 2020.

Wright, I. J., Reich, P. B., Westoby, M., Ackerly, D. D., Baruch, Z., Bongers, F., Cavender-Bares, J., Chapin, T., Cornelissen, J. H., Diemer, M., Flexas, J., Garnier, E., Groom, P. K., Gulias, J., Hikosaka, K., Lamont, B. B., Lee, T., Lee, W., Lusk, C., Midgley, J. J., Navas, M. L., Niinemets, U., Oleksyn, J., Osada, N., Poorter, H., Poot, P., Prior, L., Pyankov, V. I., Roumet, C., Thomas, S. C., Tjoelker, M. G., Veneklaas, E. J., and Villar, R.: The Worldwide Leaf Economics Spectrum, Nature, 428, 821-827, https://doi.org/10.1038/nature02403, 2004.

Wright, S. J.: The Carbon Sink in Intact Tropical Forests, Glob Chang Biol, 19, 337-339, https://doi.org/10.1111/gcb.12052, 2013.

Xiao, Z. Q., Liang, S. L., Sun, R., Wang, J. D., and Jiang, B.: Estimating the Fraction of Absorbed Photosynthetically Active Radiation from the Modis Data Based Glass Leaf Area Index Product, Remote Sensing of Environment, 171, 105-117, https://doi.org/10.1016/j.rse.2015.10.016, 2015.

Yen, V. T. and Cochard, R.: Chapter 5 - Structure and Diversity of a Lowland Tropical Forest in Thua Thien Hue Province, in: Redefining Diversity & Dynamics of Natural Resources Management in Asia, Volume 3, edited by: Thang, T. N., Dung, N. T., Hulse, D., Sharma, S., and Shivakoti, G. P., Elsevier, 71-85, https://doi.org/10.1016/B978-0-12-805452-9.00005-9, 2017.

Zanne, A. E., Lopez-Gonzalez, G., Coomes, D. A., Ilic, J., Jansen, S., Lewis, S. L., Miller, R. B., Swenson, N. G., Wiemann, M. C., and Chave, J.: Data From: Towards a Worldwide Wood Economics Spectrum [dataset], https://doi.org/10.5061/dryad.234, 2009.

Zhang, P., Hefting, M. M., Soons, M. B., Kowalchuk, G. A., Rees, M., Hector, A., Turnbull, L. A., Zhou, X., Guo, Z., Chu, C., Du, G., and Hautier, Y.: Fast and Furious: Early Differences in Growth Rate Drive Short-Term Plant Dominance and Exclusion under Eutrophication, 10, 10116-10129, https://doi.org/10.1002/ece3.6673, 2020.

Zhao, W., Tan, W., and Li, S.: High Leaf Area Index Inhibits Net Primary Production in Global Temperate Forest Ecosystems, Environ Sci Pollut Res Int, 28, 22602-22611, https://doi.org/10.1007/s11356-020-11928-0, 2021.

Ziegler, S. S.: A Comparison of Structural Characteristics between Old-Growth and Postfire Second-Growth Hemlock–Hardwood Forests in Adirondack Park, New York, U. S. A, 9, 373-389, https://doi.org/10.1046/j.1365-2699.2000.00191.x, 2000.

Zin, I. I. S. and Mitlöhner, R.: Species Composition and Stand Structure of Primary and Secondary Moist Evergreen Forests in the Tanintharyi Nature Reserve (Tnr) Buffer Zone, Myanmar, Open Journal of Forestry, 10, 445-459, https://doi.org/10.4236/ojf.2020.104028 2020.